



HAL
open science

Preservation of organic C and N isotope signatures from water column to sediments in the anoxic and ferruginous Pavin lake

Vincent Busigny, Oanez Lebeau, Didier Jézéquel, Carine Chaduteau, Sean Crowe, Magali Ader

► To cite this version:

Vincent Busigny, Oanez Lebeau, Didier Jézéquel, Carine Chaduteau, Sean Crowe, et al.. Preservation of organic C and N isotope signatures from water column to sediments in the anoxic and ferruginous Pavin lake. *Chemical Geology*, 2024, 643, pp.121814. 10.1016/j.chemgeo.2023.121814 . hal-04439647v2

HAL Id: hal-04439647

<https://u-paris.hal.science/hal-04439647v2>

Submitted on 5 Feb 2024

HAL is a multi-disciplinary open access archive for the deposit and dissemination of scientific research documents, whether they are published or not. The documents may come from teaching and research institutions in France or abroad, or from public or private research centers.

L'archive ouverte pluridisciplinaire **HAL**, est destinée au dépôt et à la diffusion de documents scientifiques de niveau recherche, publiés ou non, émanant des établissements d'enseignement et de recherche français ou étrangers, des laboratoires publics ou privés.

1 **Preservation of organic C and N isotope signatures**
2 **from water column to sediments**
3 **in the anoxic and ferruginous Pavin lake**

4
5
6 Vincent Busigny^{1,*}, Oanez Lebeau², Didier Jézéquel^{1,4},
7 Carine Chaduteau¹, Sean Crowe³, Magali Ader¹

8
9
10 ¹ Université Paris Cité, Institut de Physique du Globe de Paris, CNRS, F-75005, Paris, France

11 ² Univ Brest, CNRS, IRD, UAR3113, F29280 Plouzané, France

12 ³ Departments of Microbiology and Immunology and Earth, Ocean and Atmospheric
13 Sciences, The University of British Columbia, 2020 - 2207 Main Mall, Vancouver, British
14 Columbia V6T 1Z4, Canada

15 ⁴ UMR CARRTEL, INRAE & Université Savoie Mont Blanc, 74200 Thonon-les-Bains,
16 France

17
18
19
20
21 *For correspondence: busigny@ipgp.fr
22
23
24
25
26
27

28 **Published in** Chemical Geology:

29 Busigny V., Lebeau O., Jézéquel D., Chaduteau C., Crowe S., Ader M. (2023) Preservation of
30 organic C and N isotope signatures from water column to sediments in the anoxic and
31 ferruginous Pavin lake. Chemical Geology, <https://doi.org/10.1016/j.chemgeo.2023.121814>
32
33

34 **Abstract**

35 Organic carbon (C_{org}) and bulk nitrogen (N_{bulk}) isotope compositions (respectively $\delta^{13}C_{\text{org}}$ and
36 $\delta^{15}N_{\text{bulk}}$) of sedimentary rocks deposited in the Archean and Proterozoic eons are commonly
37 used as proxies for the biomass $\delta^{13}C_{\text{org}}$ and $\delta^{15}N_{\text{bulk}}$ values in paleo-environment and paleo-
38 ecosystem studies. Many sedimentary rocks from these eons were deposited under ferruginous
39 conditions, but it remains unknown whether C and N isotope signatures are preserved during
40 diagenetic degradation of organic matter under this chemical state. Lake Pavin, Massif Central,
41 France, is a permanently stratified freshwater lake with anoxic and ferruginous deep waters and
42 represents a unique natural site for evaluating the impact of organic matter decomposition
43 predominantly through iron redox cycling and methanogenesis. Here we present C and N
44 isotope compositions of sediment collected from traps placed at different depths in the water
45 column and from cores recovered in the anoxic zone of the lake. The $\delta^{13}C_{\text{org}}$ and $\delta^{15}N_{\text{tot}}$ values
46 in the living biomass of Lake Pavin are estimated from the shallowest sediment traps. The
47 biomass $\delta^{13}C_{\text{org}}$ values show a seasonally-controlled bimodal distribution, around -23.3 ± 1.7
48 ‰ (2σ) in September and November (organic matter produced in summer and autumn) and -
49 28.0 ± 2.6 ‰ (2σ) in April and June (organic matter produced in winter and spring). These
50 seasonal variations are attributed to variable $\delta^{13}C$ values in dissolved inorganic carbon,
51 inherited from fluctuation in the relative rates of photosynthesis *versus* respiration. The $\delta^{15}N_{\text{tot}}$
52 values are near -1 ‰ for most seasons, indicating that the dominant N source to photosynthetic
53 biomass is atmospheric N_2 .

54 Along the water column profile, organic matter mineralization released about 20 % of C and 30
55 % of N, with only moderate effects on $\delta^{13}C_{\text{org}}$ and $\delta^{15}N_{\text{tot}}$ (decreased by 1.3 and 0.4 ‰,
56 respectively). Although the water column data show significant seasonal variations, global
57 annual fluxes, estimated from regular trap collection over 15 months, are remarkably consistent
58 with the top sediment composition. In the sedimentary column, microbial degradation through
59 ferric iron reduction and methanogenesis induces a loss of 40-50% C_{org} and 50-60% N_{tot} , with
60 negligible modification of $\delta^{13}C_{\text{org}}$ and $\delta^{15}N_{\text{tot}}$. We conclude that although the C/N ratio increases
61 significantly as organic matter is degraded in the water column and in the first ~15 cm of the
62 sedimentary column, $\delta^{13}C_{\text{org}}$ and $\delta^{15}N_{\text{tot}}$ are well preserved, supporting the idea that C and N
63 isotope signatures can be reliably interpreted as tracers of primary biomass in sedimentary rocks
64 deposited in anoxic and ferruginous environments.

65

66 **1. Introduction**

67 Carbon and nitrogen are both central to life, representing the main elements in organic
68 molecules from terrestrial and extra-terrestrial materials. The evolution of carbon and nitrogen
69 biogeochemical cycles through time can be delineated from the sedimentary record back to the
70 Archean period (3.8-2.5 Ga) (*e.g.* Thomazo and Papineau, 2013; Ader *et al.*, 2016; Stüeken *et*
71 *al.*, 2016). Carbon and nitrogen isotope compositions of sedimentary organic matter have been
72 widely used for reconstructing paleobiospheric evolution (Pinti *et al.*, 2001; 2009; Stüeken *et*
73 *al.*, 2015a), variations in biological productivity (Karhu and Holland, 1996; Godfrey and
74 Falkowski, 2009; Kump *et al.*, 2011; Hashizume *et al.*, 2016), C and N sources (Beaumont and
75 Robert, 1999; Stüeken *et al.*, 2015b; Luo *et al.*, 2018) as well as the redox state of the ocean
76 (Beaumont and Robert, 1999; Garvin *et al.*, 2009; Thomazo *et al.*, 2011; Ader *et al.*, 2014;
77 Zerkle *et al.*, 2017; Kipp *et al.*, 2018; Cheng *et al.*, 2019; Koehler *et al.*, 2019).

78 The use of C and N isotope compositions as proxies of primary living organisms and/or sources
79 relies on the assumption that they are not significantly modified during diagenesis, and
80 eventually subsequent metamorphism (*e.g.* Ader *et al.*, 2016; Stüeken *et al.*, 2016; Quan and
81 Adeboye, 2021). However, organic C and N isotope signatures might be altered during
82 diagenesis through various aerobic or anaerobic microbial processes in the water column and
83 sediments. For instance, based on laboratory experiments and natural samples, early diagenetic
84 modification of organic matter was proposed to decrease $\delta^{13}\text{C}_{\text{org}}$ values by $\sim 1.5\%$, both in oxic
85 and anoxic conditions (Lehmann *et al.*, 2002), reflecting preferential removal of ^{13}C -enriched
86 organic compounds. In contrast, other studies on natural sediments demonstrated roughly
87 constant $\delta^{13}\text{C}_{\text{org}}$ values during diagenesis (*e.g.* Meyers, 1994; Freudenthal *et al.*, 2001; Chen *et*
88 *al.*, 2008; Kohzu *et al.*, 2011).

89 In the case of nitrogen, diagenetic alteration of its isotope composition has been shown to follow
90 distinct patterns for either oxic or anoxic environmental conditions. Under oxic depositional
91 conditions in the water column and/or top sediments and with long oxygen exposure-time, bulk
92 $\delta^{15}\text{N}$ values are increased by +3 to +5 ‰, as observed in both natural sites and laboratory studies
93 (Altabet *et al.*, 1999; Freudenthal *et al.*, 2001; Lehman *et al.*, 2002; Prahl *et al.*, 2003; Robinson
94 *et al.*, 2012; Gaye *et al.*, 2009). The precise origin of this increase is not completely understood
95 but is likely related to isotopic fractionation during N release, potentially through preferential
96 degradation of ^{14}N -depleted amino acids (Gaye *et al.*, 2009; Möbius *et al.*, 2010), or redox
97 reactions such as partial nitrification during diagenesis (Prokopenko *et al.*, 2006). Under anoxic
98 conditions or with high sediment depositional rates (with limited O_2 exposure), bulk $\delta^{15}\text{N}$ values

99 are generally either unmodified or slightly lowered, by less than 3 ‰ (Altabet *et al.*, 1999;
100 Lehmann *et al.*, 2002; Thunell *et al.*, 2004; Möbius *et al.*, 2010; Chen *et al.*, 2008). This
101 suggests that the N isotope compositions of sediments deposited under anoxic conditions are
102 preserved with good fidelity. However, while this has been extensively documented for
103 environments where microbial anaerobic respiration is based on nitrate and sulfate, it may not
104 be the case for other types of anoxic aquatic systems. In fact, an increase in $\delta^{15}\text{N}$ of up to 3‰
105 has been recently documented in the anoxic and alkaline Dziani Dzaha lake in which no electron
106 acceptors are present at depth and most of the organic matter is mineralized by methanogenesis
107 (Cadeau *et al.*, 2021). The preservation of $\delta^{15}\text{N}$ during early diagenesis in anoxic and
108 ferruginous systems where ferric iron is a dominant electron acceptor thus remains unknown.
109 The present work aims at filling this knowledge gap by evaluating the effect of diagenesis on
110 C and N isotope compositions of organic matter under anoxic and ferruginous conditions,
111 similar to those prevailing in the Archean and Paleoproterozoic oceans. Lake Pavin, France,
112 has been selected as a modern analog for ancient oceans because it is permanently stratified,
113 with Fe-rich deep waters where Fe(II) accumulates up to 1.2 mM (Busigny *et al.*, 2014, 2016)
114 and has been extensively studied over the past 40 years for its biodiversity (Amblard, 1986;
115 Grami *et al.*, 2011; Lehours *et al.*, 2005, 2007; Biderre-Petit *et al.*, 2011), geochemistry
116 (Michard *et al.*, 1994, Viollier *et al.*, 1997; Assayag *et al.*, 2008; Busigny *et al.*, 2014) and
117 mineralogy (Schettler *et al.*, 2007; Cosmidis *et al.*, 2014). Microbial degradation of organic
118 matter in Lake Pavin is essentially based on iron-reduction and methanogenesis (Lehours *et al.*,
119 2009; Biderre-Petit *et al.*, 2011), two processes that were probably established and possibly
120 major in Archean and Paleoproterozoic sedimentary environments (Vargas *et al.*, 1998;
121 Konhauser *et al.*, 2005; Ueno *et al.*, 2006). In the present contribution, four sediment traps were
122 set up at different depths in the water column of Lake Pavin, and collected regularly over 15
123 months. Three sediment cores were collected in the anoxic zone to examine potential lateral
124 variabilities. Carbon and nitrogen isotope compositions were measured in all samples, allowing
125 assessment of possible diagenetic modifications in the water and sediment columns, as well as
126 seasonal variations. A few plant fragments and litters collected from the lake border were also
127 analyzed and demonstrate that detrital organic matter contribution to the lake sediment is
128 negligible. Our data demonstrate for the first time that C and N isotope signatures of primary
129 biomass are faithfully transferred to sediments in a modern anoxic and ferruginous lacustrine
130 environment (although up to ~80% of organic matter is degraded). These results suggest that C
131 and N isotopic tracers can be safely used as paleo-proxies in the Precambrian rock record if
132 subsequent metamorphism is not extreme.

133

134 **2. Description of Lake Pavin**

135

136 Lake Pavin is a freshwater lake located in the Massif Central, France, 35 km to the southwest
137 of Clermont-Ferrand city (45°29.740'N - 2°53.280'E; [Fig. 1](#)). It is a volcanic lake resulting from
138 phreatomagmatism. Its geometry is quasi-circular, with a diameter of 750 m and a maximum
139 depth of 92 m. The age of Lake Pavin has been estimated to 6970 ± 60 years BP from studies
140 of volcanic products (Juvigné et Gewalt, 1987) and sediment core dating (Chapron *et al.*, 2010).
141 Lake Pavin is meromictic, *i.e.* permanently redox-stratified, with anoxic and ferruginous deep
142 waters from *ca.* 60 to 92 m depth (*i.e.* the monimolimnion), topped by oxic shallow waters from
143 0 to *ca.* 60 m (*i.e.* the mixolimnion) (Michard *et al.*, 1994; Viollier *et al.*, 1995; [Fig. 1c](#)). Over
144 the last ten years, the oxic-anoxic interface was shifted upward and is now located between 50
145 and 55 m depth (see Fig.S4 in Busigny *et al.*, 2021; Bidaud *et al.*, 2022). In the deep waters,
146 ferrous iron, $\text{Fe(II)}_{\text{aq}}$, is the main dissolved cation, with concentrations up to 1.2 mM. Dissolved
147 iron is efficiently confined below the oxic-anoxic boundary due to the formation of insoluble
148 ferric iron species, $\text{Fe(III)}_{\text{s}}$, by oxidation with O_2 and other oxidants (*e.g.*, NO_3^- , Mn(IV)) at the
149 redoxcline. This produces a significant peak of turbidity related to the formation of iron
150 particles. The $\text{Fe(III)}_{\text{s}}$ particles settle and are effectively reduced in the anoxic waters and at the
151 lake bottom by reaction with organic matter, yielding soluble $\text{Fe(II)}_{\text{aq}}$. It then diffuses upward
152 in the water column and finally is re-oxidized to Fe(III) at the redox boundary (Busigny *et al.*,
153 2016). This classic cycle is known as the “iron-wheel” (Campbell and Torgersen, 1980). The
154 lake has remarkably low sulfate concentrations ($< 20 \mu\text{M}$), and shares some similarities with
155 Archean oceans (Busigny *et al.*, 2014) - that is, high dissolved Fe(II) concentrations and low
156 levels of sulfate and sulfide. Mineral particles in the water column and sediments include mostly
157 diatom frustules, Fe-phosphate, Fe-(oxy)hydroxide, detrital silicate (clays, sanidine), and
158 siderite together with low amounts of iron sulfide (Michard *et al.*, 1994, Viollier *et al.*, 1997;
159 Schettler *et al.*, 2007; Bura-Nakic *et al.*, 2013; Cosmidis *et al.*, 2014; Busigny *et al.*, 2016). The
160 sedimentation rate estimated from radiocarbon dating on leaves from sediment cores is on
161 average 0.5 mm yr^{-1} (Chapron *et al.*, 2010).

162 The biomass of the lake is essentially composed of phytoplankton and zooplankton in shallow
163 waters, but Bacteria, Archaea, viruses and fungi are present in the whole water column (Grami
164 *et al.*, 2011). The density of the microbial community is elevated in the anoxic layer, and
165 Archaea represented the largest microbial group in the water column, with a mean

166 Archaea/Bacteria ratio around 1.5 (Lehours *et al.*, 2005). The dominant phytoplankton species
167 are alternatively diatoms (bloom in spring) and cyanobacteria (bloom in summer) (Amblard,
168 1986, 1988; Stebich *et al.*, 2005). Several studies report variations in the dominant
169 phytoplankton species with depth (Amblard, 1986) and with the seasons (Bourdier and
170 Amblard, 1987; Amblard, 1988). These are summarized in [Tables S1](#) and [S2](#) (supplementary
171 materials). Other microorganisms have been identified below the chemocline which enable
172 organic matter mineralization under anoxic conditions including methanogenic Archaea
173 (Lehours *et al.*, 2005), iron-oxidizing or -reducing Bacteria (Lehours *et al.*, 2007, 2009) and
174 sulfate-reducing Bacteria (Biderre-Petit *et al.*, 2011). The organic matter content of Lake Pavin
175 sediments is high and ranges from 4 to 18 wt% (Restituto, 1984a; Schettler *et al.*, 2007;
176 Cosmidis *et al.*, 2014).

177

178 **3. Methods**

179

180 **3.1. Samples collection**

181 *3.1.1. Water column sampling for dissolved N species analysis*

182

183 The carbon biogeochemical cycle in the water column of Lake Pavin was previously studied
184 through dissolved inorganic carbon (DIC) concentrations (Michard *et al.*, 1994) and isotope
185 compositions (Assayag *et al.*, 2008), as well as methane concentrations (Lopes *et al.*, 2011;
186 Jézéquel *et al.*, 2016). In contrast, the nitrogen biogeochemical cycle has never been
187 investigated, although dissolved NO_3^- and NH_4^+ concentrations were reported for the oxic and
188 anoxic zones respectively (Michard *et al.*, 1994). A sampling of the water column was therefore
189 conducted along a depth profile in June 2011 for measurement of N isotope compositions and
190 concentrations of nitrate (NO_3^-) and ammonium (NH_4^+). Water samples were collected using a
191 5L Niskin bottle and were subsequently filtered under N_2 atmosphere (O_2 -free), at 0.7 μm using
192 GF/F filters. The samples were stored in clean Nalgene bottles at 4°C for geochemical and/or
193 isotope analyses. For isotope analysis of NH_4^+ , water samples were acidified in the field to pH
194 < 6 with sulfuric acid (H_2SO_4) for later precipitation of ammonium sulfate salt (see section 3.2.1
195 below).

196

197 *3.1.2. Sediment traps*

198

199 Sediment traps (Uwitec, each made up of a pair of PVC tubes 60 cm long and 90 mm in diameter
200 terminated in 2L Nalgene bottles) were deployed near the center of the lake along a cable at 4
201 different depths in the water column (Fig. 1c): 25 m (oxic zone), 56 m (just above the
202 chemocline), 67 m (below the turbidity peak in the anoxic zone), and 86 m (near the lake
203 bottom). The traps were set up from March 2011 to June 2012. Five sampling campaigns were
204 organized in June 2011, September 2011, November 2011, April 2012 and June 2012. Since
205 the traps were left in place for more than 2 months, organic matter could have been partially
206 degraded within the traps. Accordingly, all traps were filled with 1 g of CuCl_2 to kill any
207 microorganisms and avoid degradation in the trap, which would represent a sampling artifact
208 (a $\text{CuCl}_2 > 2 \text{ mg/L}$ is lethal). In brief, the trap was filled with lake surface water, CuCl_2 powder
209 was dispersed in the trap and immediately dissolved, then the trap was gently moved down until
210 reaching the desired depth. The use of CuCl_2 as a poison induced dark mineral precipitation in
211 the two traps of the anoxic zone (*i.e.* 67 and 86 m depth), likely reflecting copper sulfide
212 precipitation. Since this precipitate modified the mass of sediments recovered in the anoxic trap,
213 we have not used the bulk carbon and nitrogen concentrations (in wt%) but rather used the mass
214 flux of organic carbon and nitrogen (in $\text{mg m}^{-2} \text{ day}^{-1}$), which is independent of the mass of
215 copper sulfide precipitate. It is worth noting that a few traps were settled without CuCl_2 . For
216 those one, we observed that organic matter contents were always lower than in the
217 corresponding poisoned traps while C/N ratios were higher, confirming a degradation effect
218 and thus a sample bias due to temporal evolution. This motivated the unique use of poisoned
219 traps in the present study.

220 During each sampling campaign, the traps were collected and immediately transferred to a
221 glove bag under anoxic N_2 atmosphere. The oxygen content was monitored with an Oxi 340i
222 WTW oxygen meter and was always below the detection limit (*i.e.* $< 0.1 \text{ mg/L}$). The uppermost
223 water of the traps was removed with a syringe. The residual water and sediment were mixed
224 together and homogenized before being transferred to 50 mL centrifuged tubes. The tubes were
225 shortly removed from the glove bag and immediately centrifuged on the field at 5300 rpm for
226 10 min, before being placed back in the glove bag to remove the overlying water under anoxic
227 conditions. Finally, the sediment samples were sealed under anoxic conditions and brought back
228 to the laboratory.

229

230 *3.1.3. Anoxic sediment cores*

231

232 Three different cores collected in the anoxic zone of Lake Pavin were studied to evaluate
233 potential lateral variability in the sediment depending on the depth of emplacement (Fig. 1).
234 The detailed collection procedure and sample treatment have been described in a previous
235 contribution (Busigny *et al.*, 2014). The first core (C1) was sampled at 60 m depth, near but
236 just below the redox transition zone (Michard *et al.*, 1994; Viollier *et al.*, 1995). The second
237 core (C2) was collected at 65 m depth, around the peak of sulfate reduction zone (Bura-Nakic
238 *et al.*, 2009). The last core (C6) was collected at the lake bottom, *i.e.* depth of ~ 92 m. Sediment
239 cores were transferred into a glove bag and placed under anoxic conditions (pure N₂
240 atmosphere) immediately after collection, on the field. They were processed and split into cm-
241 scale fractions along the core's vertical axis in the glove bag. The pore waters were separated
242 from the solid phases using Rhizon samplers (cut-off threshold ≈ 0.15 μm). The solid phases
243 were then frozen and transferred to the laboratory. The total thickness of sediments in each core
244 represents 10 to 14 cm. It records a time span of ~280 years, assuming a mean sedimentation
245 rate of 0.5 mm yr⁻¹ (Chapron *et al.*, 2010).

246

247 3.1.4. Plants and soil samples

248

249 Potential detrital sources in Lake Pavin sediment may derive from plant fragments and soils
250 surrounding the lake. Two main types of trees are found in Lake Pavin: beech and spruce (*e.g.*
251 Stebich *et al.*, 2005). We collected leaves, thorns and soils in June 2011, on the south-eastern
252 edge of Lake Pavin crater. All samples were placed in 50 mL Falcon® tubes and frozen
253 immediately after collection until further treatments in the laboratory. Brown beech leaves were
254 taken from broken branches on the ground. Spruce thorns were sampled directly from the trees
255 by scraping branches. Litters from two different locations on the southeast flank of the crater
256 were collected using a clean plastic spatula. They are supposed to be representative mixtures of
257 plant fragments, soil and roots.

258

259 3.2. Analytical methods

260

261 3.2.1. Analysis of dissolved N species: nitrate and ammonium

262

263 Nitrate and ammonium concentrations were measured at IPGP by colorimetry (AxFlow
264 Quattro continuous flow autoanalyzer). The limit of quantification is *ca.* 0.1 μM for both
265 species.

266 The $\delta^{15}\text{N}$ of nitrate was measured by chemical reduction of NO_3^- to NO_2^- with spongy
267 cadmium followed by reduction of NO_2^- to N_2O with azide (McIlvin and Altabet, 2005).
268 Naturally occurring NO_2^- present in the samples was previously removed by reaction with
269 sulfamic acid prior to cadmium reduction (Granger and Sigman, 2009). $\delta^{15}\text{N}$ was determined
270 on the N_2O gas produced by mass spectrometry on a Delta V Plus. Standards IAEA-N3, USGS-
271 34 and USGS-35 were used for calibration and reproducibility on replicate measurements was
272 better than 0.3 ‰.

273 For isotope analysis of NH_4^+ , water samples previously acidified with sulfuric acid were
274 evaporated at 80°C for seven days in order to precipitate ammonium sulfate (method modified
275 after Li *et al.*, 2012). $(\text{NH}_4)_2\text{SO}_4$ salts were recovered and loaded in quartz tubes, sealed under
276 vacuum, with a mix of Cu-CuO wires. The tubes were then heated to 800°C for 6 hr and slowly
277 cooled down to transform nitrogen to N_2 . Finally, the tubes were cracked under vacuum, N_2
278 was purified and analyzed in dual-inlet mode on a Delta+XP mass spectrometer. This method
279 was tested and optimized by dissolving IAEA-N1 and IAEA-N2 international standards in NH_4^- -
280 free Lake Pavin water (from 25 m depth). The results demonstrated a good yield of ammonium
281 recovery between 87 and 105 %, and $\delta^{15}\text{N}$ values of $0.3 \pm 0.5\text{‰}$ and $20.0 \pm 0.5 \text{‰}$ for IAEA-
282 N1 and -N2 standards, in good agreement with the values recommended for these two standards
283 (Gonfiantini *et al.*, 1995; Busigny *et al.*, 2005).

284

285 3.2.2. Solid samples preparation (drying, grinding)

286

287 Once in the laboratory, sediment traps and sediment core samples, as well as the two litters,
288 were dried and ground. The sealed sediment traps and the litters were loaded in a Jacomex®
289 glove box under Ar (Alphagaz 1, Air Liquide) and free of O_2 (<5 ppm), and were dried in a
290 desiccator under a vacuum of ~30 mbar. The sediment samples from cores C1 and C2 were
291 fully dehydrated by freeze-drying, while those from the core C6 were dried by evaporation at
292 50°C in an oven for 48 hr. All dried sediment samples (traps and cores) were then finely crushed
293 and homogenized in an agate mortar, while any visible plant fragments such as leaves or stems
294 were discarded. The two litter samples, brown beech leaves and spruce thorns were also crushed
295 and carefully homogenized in an agate mortar.

296

297 3.2.3. Isotopic measurements by elemental analyzer

298

299 Carbon and nitrogen concentrations and the isotope compositions of solid sediment samples
300 (traps and cores), leaves, thorns and litters were determined using a Flash EA1112 elemental
301 analyzer coupled to a Thermo Finnigan Deltaplus XP mass spectrometer via a ConFlo IV
302 interface (Thermo Fisher Scientific, Waltham, MA, United States) (Cheng *et al.*, 2019; Cadeau
303 *et al.*, 2021). Sample powders were weighed and loaded into tin capsules for analysis. Blanks
304 estimated based on empty capsules show a negligible contribution (lower than 0.5 % of the total
305 C and N amounts in the samples). Four internal standards (*i.e.* organic-rich soils and sediments),
306 calibrated against international standards, were used to calculate the $\delta^{13}\text{C}$ and $\delta^{15}\text{N}$ values of all
307 samples. The external precision on $\delta^{13}\text{C}$ and $\delta^{15}\text{N}$, determined from replicate measurements of
308 standards, was better than ± 0.34 ‰ and ± 0.30 ‰ (2σ), respectively. The long-term
309 reproducibility obtained on C and N contents, and C/N ratio, for internal standards was always
310 better than $\pm 6,7$ and 6 % relative to the measured values (2σ), respectively. Since siderite, an
311 iron carbonate, can be locally present in some layers of Lake Pavin sediments (Schettler *et al.*,
312 2007), our sample powders were decarbonated using 0.5 M HCl at room temperature for four
313 days, rinsed four times with distilled water and dried in an oven at 40°C for two days. Carbon
314 and nitrogen concentrations and isotope compositions were measured in both untreated and
315 decarbonated samples. The C concentration, $\delta^{13}\text{C}$ and $\delta^{15}\text{N}$ were undistinguishable in both cases
316 but the N concentration of decarbonated was always lower in decarbonated samples (resulting
317 in higher C/N ratios). Eight tests on sediment traps showed that decarbonation induced a loss
318 comprised between 3 to 31 % of the total nitrogen, with a mean value of 22 ± 11 % (1σ ; n=8).
319 Twelve tests on sediment samples randomly selected from the three cores gave N loss between
320 16 and 37, with a mean value of 28 ± 7 % (1σ ; n=12). Similar N alteration due to HCl treatment
321 has already been observed by Brodie *et al.* (2011a, b). Therefore, in the following sections, we
322 will only present and discuss the data obtained on untreated samples.

323

324 **4. Results**

325

326 **4.1. Dissolved nitrate and ammonium in the water column**

327 The concentrations and isotope compositions of nitrate and ammonium in Lake Pavin water
328 column are reported in [Table 1](#) and illustrated in [Figure 2](#). Ammonium is virtually absent (<0.2
329 $\mu\text{mol L}^{-1}$) in the oxic zone, but its concentration increases progressively below 50 m depth,
330 from 2.2 to 1750 μM ([Table 1](#)). Its isotope composition is remarkably constant in the anoxic
331 zone, with $\delta^{15}\text{N}$ values near 0‰, except a positive value of 4.7 ‰ near the redox boundary (56

332 m; Fig. 2). Nitrate concentrations show a very distinct behavior with a peak up to 18 $\mu\text{mol/L}$
333 between 40 and 50 m, but very low concentrations ($<0.2 \mu\text{M}$) in shallow (0-20 m) and deep
334 (below 60 m) waters. Only four water samples yielded nitrate N isotope ratios and showed
335 $\delta^{15}\text{N}_{\text{NO}_3^-}$ values increasing with depth (30 to 50 m), from -2.8 to 5.5 ‰. Similar profiles of
336 ammonium and nitrate were described in other redox stratified systems like the Black Sea,
337 Saanich Inlet, Framvaren Fjord (Velinsky *et al.*, 1991; Velinsky and Fogel, 1999) or Cariaco
338 Basin (Thunell *et al.*, 2004).

339

340 **4.2. Carbon and nitrogen fluxes and isotope compositions in sediment traps**

341 The abundances of C and N are reported as a mass flux integrated over the time (in $\text{mg m}^{-2} \text{day}^{-1}$)
342 ¹). The fluxes and isotope compositions of organic C and N deposited in the sediment traps are
343 illustrated in Figure 3 (data in Table 2). The fluxes of C and N show significant seasonal
344 variabilities, with a total range from 27 to 91 and 3.2 to 13 $\text{mg m}^{-2} \text{day}^{-1}$ respectively. The depth
345 profile variations of C and N are similar for the various seasons. Both C and N fluxes show a
346 marked decrease with depth in the water column in June 2011 and June 2012. In contrast,
347 September and November 2011 display a flux increase between the oxic and anoxic zones, but
348 a decrease at the bottom of the anoxic zone (Fig. 3). Fluxes from April 2012 were roughly
349 constant along the depth profile. Interestingly, the fluxes in June 2012 are substantially higher
350 compared to other seasons. This could reflect a bloom of diatoms subsequent to a mixing of the
351 mixolimnion (due to nutrients supply to the lake surface).

352 Carbon isotope composition shows a strong seasonal variability (Fig. 3c), with more negative
353 values in June 2011, April 2012 and June 2012 (avg. $\delta^{13}\text{C} = -28.0 \pm 2.6 \text{‰}$, 2σ , $n=12$) compared
354 to September and November 2011 (avg. $\delta^{13}\text{C} = -23.3 \pm 1.6 \text{‰}$, 2σ , $n=8$). Nitrogen isotope
355 variations differ from those of carbon isotopes. Most $\delta^{15}\text{N}$ values in sediment traps range
356 between -2 and -1 ‰, except a single value near 0‰ at 25 m depth in April 2012, and positive
357 values around +0.7‰ at all depth in June 2012 (Fig. 3d). This finding also supports a mixing
358 of the mixolimnion in April 2012, then fully recorded in the traps of June 2012. C/N ratios show
359 a moderate increase with depth for all seasons, and a total range between 6.8 and 9.7 (Fig. 3e).

360

361 **4.3. Carbon and nitrogen concentrations and isotope compositions in sediment cores**

362 The C and N data of the three sediment cores are reported in Table 3 and illustrated in Figure
363 4. The organic carbon concentration in sediment samples from core C1 (collected at 60 m depth,
364 near the redox transition zone) decreases with depth from 13.8 to 6.9 wt% (Fig. 4a, Table 3). In

365 contrast, organic C isotope compositions do not show any specific trend with depth and are
366 characterized by $\delta^{13}\text{C}_{\text{org}}$ values between -27.7 and -26.1 ‰ (avg. -26.8 ± 1.1 ‰, 2σ). Total N
367 concentration decreases significantly with depth from 1.9 to 0.8 wt% (avg. 1.2 ± 0.8 wt%, 2σ)
368 while $\delta^{15}\text{N}_{\text{tot}}$ values exhibit modest variability from -1.3 to -0.9 ‰ (avg. -1.2 ± 0.4 ‰, 2σ). The
369 C/N ratio increases moderately from 8.6 to 9.9 (avg. 9.4 ± 1.1) along the depth profile (Fig. 4e).
370 Sediments from core C2 (~65 m depth, near the peak of sulfate reduction) are remarkably
371 similar to those of the core C1 (Fig. 4). Organic carbon content decreases with depth from 13.8
372 to 6.8 wt%. The $\delta^{13}\text{C}_{\text{org}}$ values vary between -27.4 and -26.2 ‰ (avg. -26.8 ± 0.7 ‰, 2σ). Total
373 N content and isotope composition range from 0.8 to 1.9 wt% (avg. 1.2 ± 0.6 wt%, 2σ) and from
374 -1.3 to -0.6 ‰ (avg. -1.0 ± 0.4 ‰, 2σ) respectively. The C/N ratio increases with depth from
375 8.6 to 10.5 (avg. 9.8 ± 1.3).

376 Sediment from the core C6 collected at the lake bottom (92 m) is globally similar to cores C1
377 and C2 (Fig. 4a-d), except for C/N ratio (Fig. 4e). Organic C and total N concentrations in core
378 C6 both decrease with depth from 11.0 and 6.8 wt% and 1.1 to 0.6 wt%, respectively. The
379 $\delta^{13}\text{C}_{\text{org}}$ and $\delta^{15}\text{N}_{\text{tot}}$ show limited variability, with values between -27.3 to -25.2‰ (avg. $-26.6 \pm$
380 1.9 ‰) and -1.0 to 0.07 ‰ (avg. -0.6 ± 0.8 ‰) respectively. The C/N ratios in core C6 sediments
381 are significantly higher than those of the two other cores, with values from 11.3 to 13.2 (Fig.
382 4e).

383

384 **4.4. Carbon and nitrogen concentrations and isotope compositions in plant fragments** 385 **and soils**

386 The C and N concentrations and isotope compositions of the beech leaves, spruce thorns and
387 litters are given in Table 4. The mean C concentrations and $\delta^{13}\text{C}_{\text{org}}$ values are 45.9 ± 3.3 wt%
388 and -30.8 ± 0.8 ‰ for leaves, 26.5 ± 2.8 wt% and -29.8 ± 1.4 ‰ for thorns, and near 14 wt%
389 and -28 ‰ for the two litters (Table 4). The N concentrations and $\delta^{15}\text{N}_{\text{tot}}$ values average $1.3 \pm$
390 0.4 wt% and -6.7 ± 0.5 ‰ for leaves, 11 ± 0.3 ‰ and -1.2 ± 0.8 ‰ for spruce thorns, and a
391 range from 0.9 to 1 wt% and -2.4 to -3.2 ‰ for the two litters. The C/N molar ratios are high
392 compare to Lake Pavin traps and core sediments, with values averaging 40.5, 27.7 and 17 for
393 leaves, thorns and litters, respectively (Table 4). Moreover, it must be noted that these values
394 do not take into account possible degradation happening once the samples have fallen into the
395 lake.

396

397 **5. Discussion**

398 399 **5.1. Assessing the contribution of detrital carbon and nitrogen to Lake Pavin sediments**

400
401 Lake Pavin is not a closed system and allochthonous detrital components may contribute to the
402 C and N budget in the lake sediments. It is essential to determine the importance of these sources
403 before discussing the processes at play in the water column and sediments. The bedrock of Lake
404 Pavin consists of volcanic rocks, essentially rhyolites and basalts, which both contain negligible
405 amount of C and N relative to the high flux of organic matter carried by primary producers
406 thriving in the water column. Here we have not analyzed volcanic rocks from Lake Pavin but
407 for comparison, N contents in other basalts and rhyolite are in a range from 3 to 23 ppm,
408 respectively (Boocock *et al.*, 2023), about three orders of magnitude lower than N
409 concentrations in Lake Pavin sediments (*i.e.* 0.6 to 1.9 wt%, Table 3). This is thus unlikely that
410 they contribute significantly to the C and N budget in Lake Pavin sediment. A possible source
411 of allochthonous C and N could be provided by plants and/or soils surrounding the lake.
412 Although any visible leaves or stems were discarded from the sediment samples before
413 analyses, the presence of micrometer-scale fragments can hardly be ruled out. The data obtained
414 on beech leaves, spruce thorns and litters (Table 4) can be compared to those of core sediments
415 (Table 3) to explore if they can be considered as a source of organic matter in our samples. $\delta^{13}\text{C}$
416 and $\delta^{15}\text{N}$ of leaves, thorns and litters are slightly more negative than those of lake sediments,
417 with average values from -30.8 to -27.9 ‰ and -6.7 to -1.2 ‰ *versus* -26.8 to -26.5 ‰ and -1.2
418 to -0.6 ‰, respectively (Tables 3 and 4). The greatest difference is observed for C/N ratio, with
419 values of 9.4 to 12.3 in core sediments (Table 3) *versus* 16.3 to 40.5 (Table 4). The low C/N
420 ratios of lake sediments are better explained by a dominant contribution of organic matter from
421 the water column, as also recorded in sediment traps (Table 2). The sediments from the lake
422 bottom (core C6, 92m, Table 3) has a C/N ratio (12.3) relatively close to those of litters (16.3-
423 17) but the $\delta^{15}\text{N}$ values of these sediments are markedly heavier (-0.6 ‰) and contrast with the
424 lighter values measured in litters (-2.4 to -3.2 ‰). Accordingly, we can reasonably assume that
425 our lake sediment samples contain only a minor proportion of allochthonous organic matter but
426 a dominant biomass from primary producers of the water column. This conclusion is also
427 consistent with further calculation showing that global annual sediment particles recorded in
428 traps are consistent with top core sediment values (see section 5.4 below).

429

430 **5.2. Carbon and nitrogen isotope signatures of primary biomass in Lake Pavin**

431 In this section, we examine the origin of C and N isotope compositions of the primary biomass
432 of Lake Pavin. These isotope compositions depend essentially on the composition of the
433 chemical compounds that are assimilated by living organisms (*i.e.* sources of C and N), as well
434 as isotope fractionations related to the assimilation processes. The primary biomass in Lake
435 Pavin is essentially produced between 10 and 15 m depth in the water column (Amblard, 1986,
436 1988), identified on depth profile by the peaks of O₂ production and turbidity (Assayag *et al.*,
437 2008; Busigny *et al.*, 2016). Thus, the most appropriate and best preserved samples recording
438 the primary biomass are the sediment traps collected at 25 m depth.

439

440 *5.2.1. Origin of the C isotopic composition of organic matter in Lake Pavin*

441 The C isotope composition of organic matter in sediment traps from 25 m depth shows a
442 bimodal distribution, closely tied to seasonal variations, with mean $\delta^{13}\text{C}$ values at -23.3 ± 1.6
443 ‰ (2σ , $n=8$) in September and November (organic matter produced in summer and autumn)
444 and -28.0 ± 2.6 ‰ (2σ , $n=12$) in April and June (organic matter produced in winter and spring)
445 (Fig. 3c). This seasonal difference may reflect a change in (i) the carbon isotope fractionation
446 between dissolved CO₂ and organic matter (noted as ϵ_p , the subscript “p” standing for
447 photosynthesis; *e.g.* Hayes, 2001) and/or (ii) the $\delta^{13}\text{C}$ of dissolved CO₂ (*i.e.* source of C in
448 biomass). These two possibilities are examined below.

449 We first estimate the values of ϵ_p for the two distinct periods (summer-autumn *vs.* winter-
450 spring) to evaluate if they differ significantly and could explain the $\delta^{13}\text{C}$ offset of ~ 4.7 ‰ (Fig.
451 3c). Variable ϵ_p values could for instance arise due to differences in the primary producing
452 organisms between the seasons. The biomass in the upper water column of Lake Pavin is
453 composed of phytoplankton and zooplankton. The dominant phytoplankton species are diatoms
454 (present all year long, and characterized by a bloom in spring) and cyanobacteria, which bloom
455 in summer (Amblard, 1986, 1988, Stebich *et al.*, 2005). Previous studies demonstrated a vertical
456 stratification of phytoplankton species living during a single period of time (Amblard, 1986;
457 see compilation in Table S1), as well as a seasonal variability of phytoplankton (Bourdier and
458 Amblard, 1987; Amblard, 1988; see Table S2). The determination of ϵ_p values in Lake Pavin is
459 not straightforward. While C isotope data of organic matter are available from the sediment
460 traps collected at 25 m depth, the isotope composition of CO₂ dissolved in the water column
461 ($\delta^{13}\text{C}_{\text{CO}_2}$) has not been determined in the present work. An approximation $\delta^{13}\text{C}_{\text{CO}_2}$ can be
462 calculated from previously published isotope compositions of dissolved inorganic carbon (DIC)

463 (Assayag *et al.*, 2008). In Lake Pavin water column, DIC is dominated by the chemical species
 464 HCO_3^- because the pH is comprised between 6 and 9 (Assayag *et al.*, 2008). Thus, the isotope
 465 compositions of DIC and HCO_3^- can reasonably be considered as identical (*i.e.* $\delta^{13}\text{C}_{\text{DIC}} =$
 466 $\delta^{13}\text{C}_{\text{HCO}_3^-}$). Then, the isotope composition of dissolved CO_2 ($\delta^{13}\text{C}_{\text{CO}_2}$) in equilibrium with
 467 HCO_3^- can be estimated from the relation between the isotope fractionation $\varepsilon_{\text{CO}_2-\text{HCO}_3^-}$ and
 468 temperature (Mook *et al.*, 1974):

$$469 \quad \varepsilon_{\text{CO}_2-\text{HCO}_3^-} = 24.12 - \frac{9866}{T+273} \sim \delta^{13}\text{C}_{\text{CO}_2} - \delta^{13}\text{C}_{\text{HCO}_3^-} \quad (1)$$

470 where the temperature T is expressed in °C. Equation 1 can also be written as:

$$471 \quad \delta^{13}\text{C}_{\text{CO}_2} \sim \delta^{13}\text{C}_{\text{HCO}_3^-} + 24.12 - \frac{9866}{T+273} \quad (2)$$

472 The isotope composition of dissolved CO_2 can be assessed for any temperature and isotope
 473 composition of HCO_3^- (equal to DIC). Using the temperature and $\delta^{13}\text{C}_{\text{DIC}}$ values measured
 474 previously in the zone of maximum primary productivity (surface to 15-20 m), we estimated a
 475 range of $\delta^{13}\text{C}_{\text{CO}_2}$ for summer and winter based on data from July 2004 and November 2002
 476 respectively (Assayag *et al.*, 2008). The considered $\delta^{13}\text{C}_{\text{HCO}_3^-}$ and temperatures ranged from -
 477 2.7 to 0.5‰ and 4.8 to 9.7°C in November 2002, and from 1.0 to 4.4‰ and 4.5 to 16.6°C in
 478 July 2004, respectively (Table S3). The calculated $\delta^{13}\text{C}_{\text{CO}_2}$ values are on average -8.3 ± 0.8 ‰
 479 ($n=8$) for summer and -11.7 ± 1.1 ‰ ($n=7$) for winter (Table S3). If these values can be extended
 480 in time (an assumption confirmed from unpublished DIC data monitored over years by IPGP
 481 teams), the C isotope fractionation (ε_p) between dissolved CO_2 and organic matter can be
 482 calculated by combining these $\delta^{13}\text{C}_{\text{CO}_2}$ values with our data on organic matter from the sediment
 483 traps at 25 m as:

$$484 \quad \varepsilon_p = \delta^{13}\text{C}_{\text{CO}_2} - \delta^{13}\text{C}_{o.m.} \quad (3)$$

485 The estimated isotope fractionation ε_p associated to photosynthesis is about 14.0 ± 1.0 ‰ in
 486 summer and 15.0 ± 2.1 ‰ in winter, both values being in the range determined for diatoms
 487 under various experimental conditions (*e.g.* Riebesell *et al.*, 2000). The similarity between these
 488 two estimates (within uncertainty) implies that the seasonal variability observed in organic
 489 matter $\delta^{13}\text{C}$ (a ~ 4.7 ‰ offset between -23.3 ‰ in summer-autumn vs. -28.0 ‰ in winter-spring)
 490 cannot be simply explained by different C isotope fractionation related to temperature variations
 491 and/or differences in primary producing organisms. Therefore, it more likely reflects a seasonal
 492 change in the C isotope composition of DIC. This change might be related to variable
 493 photosynthetic activity in time, with higher activity in summer and lower activity in winter.
 494 Seasonal control of C isotope composition in organic matter has already been observed (*e.g.*

495 Gu and Schelske, 1996), with sometimes large variations like in Lake Lugano, where $\delta^{13}\text{C}_{\text{org}}$
496 values are around -35 and -25 ‰ in winter and summer respectively (Bernasconi *et al.*, 1997).
497 Large isotopic variations between seasons were interpreted as resulting from a combination of
498 primary productivity level, changes in the carbonate chemistry (specifically controlled by pH
499 variations) and isotope fractionation related to photosynthesis (Bernasconi *et al.*, 1997). It was
500 not possible to establish a dominant parameter because of the strong vertical and temporal
501 variability in the water column. Our variations observed in Lake Pavin can be fully explained
502 by seasonal changes in the isotope compositions of the CO_2 assimilated during primary
503 productivity, itself probably resulting from changes in the seasonal changes in the ratio of
504 photosynthesis to respiration.

505

506 5.2.2. *Origin of the N isotope signature of organic matter in Lake Pavin*

507 In the sediment traps collected at Lake Pavin, the $\delta^{15}\text{N}_{\text{tot}}$ values are near -1 ‰ for all seasons
508 (Fig. 3d), except in April 2012 (0.1 ‰ at 25 m depth) and June 2012 (~ +1 ‰ at all depth). The
509 N isotope composition of organic matter can help to decipher the N sources assimilated by
510 living organisms. Autotrophic organisms can assimilate four different sources of inorganic N
511 in the form of either dinitrogen (N_2), nitrite (NO_2^-), nitrate (NO_3^-) or ammonium (NH_4^+). Nitrate
512 and ammonium are usually the first chemical species to be used because their assimilation
513 requires less energy than N_2 , for which the triple bond is hard to break, and nitrite
514 concentrations are generally very low in natural system (Quan and Falkovski, 2009). In Lake
515 Pavin, NH_4^+ is present in anoxic deep waters, with an increasing concentration from the redox
516 boundary to the lake bottom. Similar profiles have been observed in other redox stratified
517 aquatic systems like the Black Sea, Saanich Inlet or Framvaren Fjord (*e.g.* Velinsky *et al.*, 1991;
518 Velinsky and Fogel, 1999). Nitrate is virtually absent (< 0.2 μM) in surface waters, down to 20
519 m depth. It then shows a moderate peak (up to 18 μM) between 40 and 50 m depth (Fig. 2),
520 likely reflecting some degree of organic matter mineralization by oxygen in this interval of the
521 water column. This could explain the progressive increase of $\delta^{15}\text{N}$ with depth from -2.8 to +5.5
522 (Fig. 2b). Near the redox boundary, both NO_3^- and NH_4^+ concentrations decrease, which may
523 indicate a consumption by denitrification and anammox processes (Galbreith *et al.*, 2008;
524 Sigman *et al.*, 2009). Part of the nitrate accumulating between 50 and 56 m may result from the
525 oxidation of ammonium diffusing upward in the water column (Fig. 2). Recent studies
526 suggested that dissimilatory nitrate reduction to ammonium (DNRA) could be an important
527 biological mechanism in ferruginous systems, where aqueous Fe(II) could act as an electron

528 donor for nitrate reduction (*e.g.* Michiels *et al.*, 2017). Although we cannot exclude that this
529 mechanism is present in Lake Pavin, it is unlikely a dominant process near the redox interface
530 for the following reasons: first, nitrate is present in the depth zone where oxygen is still available
531 and no ammonium is detected, and second, Fe(II) is oxidized and trapped well below the depth
532 of nitrate accumulation.

533 The major biomass production in surface waters of Lake Pavin cannot be sustained by NO_3^-
534 and/or NH_4^+ because none is present. They may only occasionally be brought to surface waters
535 by mixing with deep waters (*e.g.* from 30 to 60 m; Fig. 2a). Nitrogen is thus likely a limiting
536 nutrient in Lake Pavin surface waters (like phosphorus, which is trapped and sequestered in the
537 monimolimnion by Fe-oxyhydroxide precipitation; *e.g.* Cosmidis *et al.*, 2014; Busigny *et al.*,
538 2016) and N_2 represents the main N source for this biomass. The biological fixation of N_2 by
539 autotrophic organisms under either oxic or anoxic conditions is associated with low N isotope
540 fractionations ($< 3\text{‰}$; Minagawa and Wada, 1986; Fogel and Cifuentes, 1993). Consequently,
541 organic matter produced by N_2 -fixation generally shows $\delta^{15}\text{N}$ close to 0‰ , similar to
542 atmospheric values. Laboratory cultures of N_2 -fixing organisms in Fe-rich medium
543 demonstrated slightly negative N isotope compositions of organic matter down to -3‰ (Zerkle
544 *et al.*, 2008), and in some cases with extreme values down to -7‰ when other metal co-factors
545 are present (Zhang *et al.*, 2014). In Lake Pavin, the $\delta^{15}\text{N}$ of organic matter collected in sediment
546 traps ($\sim -1\text{‰}$; Fig. 3d) suggests that the dominant N source for biomass corresponds to
547 atmospheric N_2 dissolved in surface waters. Rare mixing events of surface waters with waters
548 from 30 to 60 m depth, like in January 2012, can inject some NO_3^- in shallow waters, and
549 potentially also some NH_4^+ . Nitrate and ammonium can then be assimilated and produce
550 positive $\delta^{15}\text{N}$ values in biomass (*e.g.* $+1\text{‰}$ in June 2012). Such assimilation would require to
551 be complete (or almost) since nitrate or ammonium assimilation processes both favor ^{14}N over
552 ^{15}N , and a partial assimilation would impart negative $\delta^{15}\text{N}$ values in biomass. A complete
553 assimilation is not reasonable given the high primary productivity in Lake Pavin. The average
554 $\delta^{15}\text{N}$ value of dissolved NO_3^- is 2.4‰ , suggesting active denitrification/anammox near the
555 redox interface. Ammonium measured near the redox interface (56 m depth) has a $\delta^{15}\text{N}$ value
556 of $+4.7\text{‰}$. A complete consumption of NO_3^- and NH_4^+ after mixing of the upper waters,
557 together with some degree of N_2 -fixation, could easily account for the positive $\delta^{15}\text{N}$ values
558 observed in April (at 25 m) and June 2012 (all depths) (Fig. 3d). Changes of N sources (from
559 NH_4^+ to NO_3^- and/or to N_2) have already been described for other systems like Lake Kinneret,
560 Israel (Hadas *et al.*, 2009), where strong seasonality effects are the main cause of these changes.

561 However, N isotope signature dominantly controlled by N₂-fixation is rarely observed in
562 modern environments but more common in the sedimentary record for instance during oceanic
563 anoxic events (OAE; Rau *et al.*, 1987; Jenkyns *et al.*, 2007; Junium and Arthur, 2007) and some
564 Archean periods (Stüeken *et al.*, 2015; Stüeken and Buick, 2018).

565

566 **5.3. Diagenetic modifications in the water column**

567 The impact of organic matter degradation in the water column of Lake Pavin can be evaluated
568 by comparing the fluxes of C and N, and the $\delta^{13}\text{C}_{\text{org}}$ and $\delta^{15}\text{N}_{\text{tot}}$ values recorded in the different
569 sediment traps along the depth profile. Although these four parameters show relatively
570 consistent values, they are characterized by significant seasonal variabilities (Fig. 3). Rather
571 than describing detailed seasonal variations, we present here a global perspective based on
572 annual fluxes and isotope compositions in order to convey the main trends with respect to
573 diagenetic modifications. This approach has the advantage of providing average values to be
574 compared to sediment core data (see section 5.3 below).

575 We calculated the annual fluxes of C, N, as well as average $\delta^{13}\text{C}_{\text{org}}$ and $\delta^{15}\text{N}_{\text{tot}}$ values (weighted-
576 average considering the respective fluxes of C and N) for the sediment traps at 25 m (oxic zone),
577 56 m (just above the chemocline), 67 m (below the turbidity peak in the anoxic zone), and 86
578 m depth (near the lake bottom). The data are summarized in Table 5. The annual fluxes of C
579 and N show a decrease from shallow to deep sediment traps, with values from 17.8 to 14.3 and
580 2.7 to 1.9 g m⁻² yr⁻¹, respectively (Table 5). This decrease corresponds to a loss of 23.8 ± 1.9 %
581 of organic carbon and 29.6 ± 2.3 % of nitrogen, indicating that N is more efficiently mineralized
582 than C (translated to an increase of C/N ratio of 8.2 ± 0.5 %; Fig. 3). The mean annual $\delta^{13}\text{C}_{\text{org}}$
583 decreases with depth by ~ 1.3 ‰ (-25.2 to -26.5 ‰), while $\delta^{15}\text{N}_{\text{tot}}$ also decreases but by only 0.4
584 ‰ (-0.5 to -0.9 ‰; Table 5). In detail, the isotopic modifications appear to take place mostly in
585 the shallow oxic zone, while the deep sediment traps of the anoxic zone have identical values.
586 Intra-seasonal variabilities are not discussed here for simplicity, but if considered, they lead to
587 similar conclusions for the evolution of C and N isotope compositions. Previous comparison of
588 $\delta^{15}\text{N}$ values in sediment traps and surface sediments of the modern well-oxygenated ocean
589 shows variably altered signatures, with enrichment in heavy isotope up to 6 ‰ (Altabet and
590 François, 1994). Alteration of $\delta^{15}\text{N}$ values is a function of water depth and likely reflects oxygen
591 exposure time (see review in Robinson *et al.*, 2012). In the open ocean under low sedimentation
592 rate, the alteration can be significant. In contrast, under high sedimentation rate, high export
593 production, low O₂, and good organic matter preservation, for instance in settings near
594 continental margins, the alteration of the N isotope composition is minimal. In the stratified

595 euxinic Cariaco basin, Thunell *et al.* (2004) observed a moderate decrease of $\delta^{15}\text{N}$ (by 0.7‰)
596 between sinking particles and surface sediments. The direction and magnitude of this variation
597 is similar to the one observed here in Lake Pavin (~0.4‰). A larger decrease of $\delta^{15}\text{N}$ (3‰) was
598 sometimes reported in sinking particles like at the North Atlantic Bloom Experiment site, which
599 was interpreted as selective removal of ^{15}N -enriched compounds, or addition of ^{14}N -enriched
600 organic material (Altabet *et al.*, 1991). In the case of Lake Pavin particulate matter, the
601 combined loss of C and N with depth is better explained by a removal than an addition of
602 organic compounds.

603

604 **5.4. Diagenetic modifications in sediments**

605 Previous studies of diagenetic evolution in oceanic or lacustrine environments, under the
606 influence of O_2 , NO_3^- and SO_4^{2-} , illustrated limited modification of C isotope composition (*e.g.*
607 Freudenthal *et al.*, 2001; Kohzu *et al.*, 2011a) but contrasted N isotope results (Sachs and
608 Repeta, 1999; Freudenthal *et al.*, 2001; Lehmann *et al.* 2002; Kohzu *et al.*, 2011b). Analysis of
609 a 30 cm long sediment core collected near the Canary Islands in eastern Atlantic Ocean revealed
610 that $\delta^{13}\text{C}_{\text{org}}$ and $\delta^{15}\text{N}_{\text{tot}}$ were poorly modified during diagenesis with variations lower than 1‰
611 (Freudenthal *et al.*, 2001). Detailed analysis of C isotope composition in sediments from Lake
612 Kasumigaura, Japan, also show a good preservation, with $\delta^{13}\text{C}_{\text{org}}$ of 15 cm-long sediment cores
613 varying within $\pm 0.6\%$ (Kohzu *et al.*, 2011a). In contrast, a companion study on the same
614 samples determined significant N isotope modifications, with increasing $\delta^{15}\text{N}_{\text{tot}}$ values in the 4
615 cm top sediments but decreasing values in deeper sediments (Kohzu *et al.*, 2011b). The
616 diagenetic modifications of sediments are usually believed to increase $\delta^{15}\text{N}$ values under well-
617 oxygenated conditions, but decrease under anoxic conditions (Sachs and Repeta, 1999;
618 Lehmann *et al.* 2002). The $\delta^{15}\text{N}$ decrease in Lake Kasumigaura sediments may reflect either
619 preferential degradation of ^{15}N -enriched components (like the chitin fraction; *e.g.* Brahney *et*
620 *al.*, 2006) or addition of ^{14}N -enriched organic matter by bacterial growth from dissolved
621 ammonium in porewater sediments (Kohzu *et al.*, 2011b).

622 In Lake Pavin, the diagenetic modifications of organic C and N can be addressed from the depth
623 profile of the three sediment cores collected at 60, 65 and 92 m depth (Fig. 4). Before discussing
624 the chemical and isotope evolutions within the cores, it is interesting to compare the sediment
625 surface (top core) to the global annual values calculated in section 5.2. The average annual
626 sediment deduced from sediment traps have $\delta^{13}\text{C}_{\text{org}}$, $\delta^{15}\text{N}_{\text{tot}}$ and C/N values of -26.5 ‰, -0.9 ‰
627 and 8.4 (Table 5). These values are undistinguishable from those of the top core sediments (Fig.

628 4, Table 5), which validates both measurements and calculations. Moreover, it provides a
629 reliable assessment of the starting material, before diagenetic modifications in the sedimentary
630 pile. Part of the total nitrogen in solid sediment is possibly carried as NH_4^+ substituting for K^+
631 in clay minerals (e.g. Müller, 1977). However, clay content in Lake Pavin is particularly low.
632 The sediment is dominated by diatom frustules ($> 40\%$ SiO_2 in bulk; Schettler *et al.*, 2007),
633 vivianite (iron phosphate), and organic matter ($>10\%$ in the top sediment; Table 3). Aluminum
634 content is always lower than 2.5 wt% (Schettler *et al.*, 2007) and generally around 1 wt%
635 (Busigny *et al.*, 2014), which translates to a maximum K content of 1.3 wt% (considering K/Al
636 molar ratio of 0.37 ± 0.07 , 2SD, $n=14$; data from Busigny *et al.*, 2014). Assuming a relation
637 between K^+ and NH_4^+ similar to the one established for oceanic sediments (Müller, 1977), the
638 maximum NH_4^+ content in clay minerals of Lake Pavin sediments can be estimated to 100 ppm.
639 This value is two orders of magnitude lower than the ~ 1 wt% measured for total N in bulk
640 (Table 3), demonstrating that organic matter is the main N carrier in Lake Pavin sediments.
641 The three sediment cores, C1 (60 m, near the redox transition zone), C2 (65 m, near the peak
642 of sulfate) and C6 (92 m, lake bottom), show consistent evolution in the sedimentary column,
643 with a decrease in C and N concentrations but no specific trends in $\delta^{13}\text{C}_{\text{org}}$ and $\delta^{15}\text{N}_{\text{tot}}$ values
644 (Fig. 4). Overall 40-50 % C and 50-60 % N were lost during this diagenetic evolution. The
645 $\delta^{13}\text{C}_{\text{org}}$ values of cores C1, C2 and C6 average -26.8 ± 1.1 ‰ (2σ , $n=6$), -26.8 ± 0.7 ‰ (2σ ,
646 $n=12$), -26.5 ± 1.9 ‰ (2σ , $n=5$), while $\delta^{15}\text{N}_{\text{tot}}$ values are -1.2 ± 0.4 ‰ (2σ , $n=6$), -1.0 ± 0.4 ‰
647 (2σ , $n=12$), -0.6 ± 0.8 ‰ (2σ , $n=5$), respectively (Table 3). In each core, both $\delta^{13}\text{C}_{\text{org}}$ and $\delta^{15}\text{N}_{\text{tot}}$
648 can be regarded as constant within uncertainty. Since oxygen, nitrate and sulfate are absent in
649 the sediment, the decrease of particulate C and N concentrations with depth can only be
650 attributed to organic matter mineralization by microbial reduction of Fe(III) phases such as iron
651 (oxy)hydroxides and ferric phosphate (Busigny *et al.*, 2014; Cosmidis *et al.*, 2014), and
652 methanogenesis (Lehours *et al.*, 2005; Borrel *et al.*, 2011; Biderre-Petit *et al.*, 2011; Lopes *et*
653 *al.*, 2011). Importantly, the relative constancy of $\delta^{13}\text{C}_{\text{org}}$ and $\delta^{15}\text{N}_{\text{tot}}$ observed here indicates that
654 these metabolic degradation pathways (Fe(III)-based and methanogenesis) do not impact the C
655 and/or N isotope compositions of organic matter, even though $\sim 50\%$ of the initial organic
656 matter have been lost. Nevertheless, it must be pointed out that our samples represent only the
657 12 cm top-sediments and this conclusion will need to be tested further in longer sediment cores.
658 An intriguing result in Lake Pavin sediments is the difference between C/N ratios of 8.6-10.5
659 in cores C1 and C2 and 11.3-13.2 in core C6. The origin of this difference is not clear but may
660 reflect a specific degradation mechanism of organic matter at the lake bottom. A possibility is

661 for instance that sediments from C1 and C2 cores were more impacted by Fe(III) reduction, due
662 to the proximity to the redox boundary, while the lake bottom sediments mostly involved
663 methanogenic degradation. Indeed, ferric iron particles are partly reduced in the water column
664 and are thus less abundant in the deepest sediments, after a longer travel when sinking in the
665 water column (Cosmidis *et al.*, 2014; Busigny *et al.*, 2016). The fate of ammonium produced
666 by organic matter degradation in sediment can hardly be discussed from our Lake Pavin data
667 since no ammonium concentrations and/or isotope compositions were determined in the
668 sediment porewater profiles. However, we note that $\delta^{15}\text{N}_{\text{NH}_4^+}$ in the deepest sample of the water
669 column sample (90 m) is -0.36‰ , a value undistinguishable from the average ($-0.6 \pm 0.8\text{‰}$) of
670 lake bottom sediment (92 m, Table 3). This suggests that most ammonium released from
671 sediment is unchanged and simply diffuses towards the water column although a minor part of
672 it might be oxidized to N_2 or NO_2^- by Fe(III)-user microorganisms, as observed in wetland soils
673 (Clement *et al.*, 2005) or tropical upland soil slurries (Yang *et al.*, 2012).

674

675 **5.5. Implications for paleo-environment and –ecosystem reconstruction**

676 In Lake Pavin water column, organic matter mineralization reached $\sim 20\%$, while $\delta^{13}\text{C}_{\text{org}}$ and
677 $\delta^{15}\text{N}_{\text{tot}}$ decrease by only ~ 1.3 and 0.4‰ , respectively (Table 5). In sediments, about 50% of the
678 initial organic matter was mineralized (on the top of the 20% that already happened in the water
679 column) but $\delta^{13}\text{C}_{\text{org}}$ and $\delta^{15}\text{N}_{\text{tot}}$ remained roughly constant, within uncertainty. This indicates
680 that organic matter degradation based on ferric minerals and/or methanogenesis does not
681 modify significantly C and N isotope compositions in anoxic and ferruginous environments.
682 Such limited modifications are consistent with previous results obtained for other anoxic
683 settings where organic matter degradation was based on nitrate or sulfate reduction processes
684 (*e.g.* Altabet *et al.*, 1999; Lehmann *et al.*, 2002; Thunell *et al.*, 2004; Möbius *et al.*, 2010; Chen
685 *et al.*, 2008). Therefore, while strong isotopic effects are observed for oxic degradation of
686 organic matter (*e.g.* Robinson *et al.*, 2012), sediments deposited under any type of anoxic
687 environment should preserve their C and N isotope compositions, and be safely used as paleo-
688 recorders of past C and N biogeochemical cycles. This conclusion is important specifically for
689 isotope studies of sedimentary rocks from the Archean and Proterozoic eons, as well as anoxic
690 periods from the Phanerozoic (*e.g.* oceanic anoxic events, sapropels, thermal maximum periods
691 like PETM or MECO).

692 In the rock record, metamorphic processes can eventually modify $\delta^{13}\text{C}$ and $\delta^{15}\text{N}$ values.
693 However, previous studies on coals of variable metamorphic grades demonstrated that $\delta^{15}\text{N}$ is

694 well preserved although N content decreases and C/N ratio increases (Ader *et al.*, 1998; Boudou
695 *et al.*, 2008). In the case of N present as ammonium (NH_4^+) substituting for K^+ in the structure
696 of silicate minerals, metamorphism can lead to a partial N loss associated to an increase in $\delta^{15}\text{N}$
697 values by a few per mil in the residual rock (Bebout and Fogel, 1992; Mingram and Brauer,
698 2001; Busigny and Bebout, 2013). The potential effect of metamorphism can generally be
699 avoided by studying rocks of low metamorphic grade, such as prehnite–pumpellyite or
700 greenschist facies (*e.g.* Stüeken *et al.*, 2015, 2016; Luo *et al.*, 2018).

701 The isotope composition of different N species in Lake Pavin are consistent with a typical
702 model of redox stratified system, where the dissolved NO_3^- and NH_4^+ , respectively in the oxic
703 and anoxic zones, are largely lost at the redox interface via denitrification and anammox
704 processes. Diazotrophic organisms living in the photic zone therefore consume dissolved N_2 to
705 counterbalance the absence or limited availability of NO_3^- . The low $\delta^{15}\text{N}$ values observed in
706 biomass ($\sim -1\text{‰}$) are similar to those measured in organic matter-rich sediments deposited
707 during anoxic marine periods such as Oceanic Anoxic Event (OAE) and sapropels (Rau *et al.*,
708 1987; Jenkyns *et al.*, 2007; Junium and Arthur, 2007) and in some sedimentary rocks deposited
709 in the Archean and Paleoproterozoic (Stüeken *et al.*, 2015; Luo *et al.*, 2018; Koehler *et al.*,
710 2019). These results are however distinct from redox stratified marine systems like the Black
711 Sea or Cariaco basin, where positive $\delta^{15}\text{N}$ values of sediments (essentially between 3 and 7‰)
712 can be attributed to a biomass assimilating partially-denitrified NO_3^- (Thunell *et al.*, 2004;
713 Fulton *et al.*, 2012; Quan *et al.*, 2013). In the specific case of the Black Sea, redox conditions
714 have changed with time due to rise and fall of sea level related to glacial-interglacial periods.
715 The Black Sea is known to have alternated between anoxic, saline waters in high level (*i.e.*
716 connection with the Mediterranean Sea), and oxic, less saline conditions (dominated by
717 freshwaters) in low sea level. Quan *et al.* (2013) showed that $\delta^{15}\text{N}$ in sediments are similar
718 under oxic and anoxic periods (3 to 4‰) but increase to higher values ($\sim 6\text{‰}$) during glacial-
719 interglacial transition periods. This increase in $\delta^{15}\text{N}$ was attributed to partial denitrification
720 under suboxic conditions, and subsequent transfer of the isotope signature of residual nitrate to
721 biomass. Although the lowest $\delta^{15}\text{N}$ values of the Black Sea sediment can be explained by a
722 stronger influence of N_2 -fixing organism, these values are still positive and require some
723 degrees of ^{15}N -enriched nitrate or ammonium consumption. The Black sea and Cariaco basin
724 are often considered as analogues for stratified oceanic systems and taken as references for
725 interpretation of paleo-environments. However, they are not really suitable analogues for the
726 global N cycle because they are fed by external sources of NO_3^- . Lake Pavin may represent a

727 better analog and illustrates, in a natural system, some of the theoretical concepts developed for
728 OAE and Precambrian ocean.

729

730 **6. Conclusion**

731 We present the first assessment of organic matter C and N isotope evolution during diagenesis
732 in anoxic and ferruginous sedimentary system, as illustrated by the case of Lake Pavin. Apart
733 from significant seasonal variability affecting C isotope compositions, $\delta^{13}\text{C}_{\text{org}}$ and $\delta^{15}\text{N}_{\text{tot}}$ in
734 sediment traps along the water column profiles are only moderately different by 1.3 and 0.4 ‰,
735 respectively. Moreover, the average sediment traps collected in the anoxic zone are remarkably
736 similar to the top sediments at the lake bottom. In the sedimentary column, $\delta^{13}\text{C}_{\text{org}}$ and $\delta^{15}\text{N}_{\text{tot}}$
737 do not show any specific evolution with depth and can be regarded as constant. Lake Pavin data
738 therefore demonstrate that organic matter degradation in anoxic and ferruginous conditions
739 preserve $\delta^{13}\text{C}_{\text{org}}$ and $\delta^{15}\text{N}_{\text{tot}}$ of the primary biomass, with only minor modifications. It confirms
740 previous assumptions of Archean and OAE studies that $\delta^{13}\text{C}_{\text{org}}$ and $\delta^{15}\text{N}_{\text{tot}}$ can be used as
741 reliable paleo-proxy of biomass and environmental conditions.

742

743 **Acknowledgment**

744 This work was partly funded by the INSU-INTERRVIE program of the CNRS. Colleagues
745 from GIS team in IPGP are thanked for fruitful discussions. Guillaume Landais is
746 acknowledged for technical assistance. Laura Bristow helped with the determination of the N
747 isotopic composition of nitrate. Christelle Busigny is thanked for her great support during all
748 field trips to Lake Pavin. Fieldwork was facilitated by permanent support from Besse
749 municipality, in particular Marie Léger from the heritage department. We thank Eva Stüeken
750 and an anonymous reviewer for constructive reviews, and Hailiang Dong for handling the
751 manuscript.

752

753 **References**

- 754 Ader, M., 1998. Nitrogen isotopic composition of ammonium-rich illite in anthracites and
755 organic-rich shales from Eastern Pennsylvania. *Mineralogical Magazine* 62A, 13–14.
756 <https://doi.org/10.1180/minmag.1998.62A.1.07>
- 757 Ader, M., Sansjofre, P., Halverson, G.P., Busigny, V., Trindade, R.I.F., Kunzmann, M.,
758 Nogueira, A.C.R., 2014. Ocean redox structure across the Late Neoproterozoic Oxygenation
759 Event: A nitrogen isotope perspective. *Earth and Planetary Science Letters* 396, 1–13.
760 <https://doi.org/10.1016/j.epsl.2014.03.042>
- 761 Ader, M., Thomazo, C., Sansjofre, P., Busigny, V., Papineau, D., Laffont, R., Cartigny, P.,

762 Halverson, G.P., 2016. Interpretation of the nitrogen isotopic composition of Precambrian
763 sedimentary rocks: Assumptions and perspectives. *Chemical Geology* 429, 93–110.
764 <https://doi.org/10.1016/j.chemgeo.2016.02.010>

765 Altabet, M.A., Deuser, W.G., Honjo, S., Stienen, C., 1991. Seasonal and depth-related changes
766 in the source of sinking particles in the North Atlantic. *Nature* 354, 136–139.
767 <https://doi.org/10.1038/354136a0>

768 Altabet, M.A., Francois, R., 1994. Sedimentary nitrogen isotopic ratio as a recorder for surface
769 ocean nitrate utilization. *Global Biogeochem. Cycles* 8, 103–116.
770 <https://doi.org/10.1029/93GB03396>

771 Altabet, M.A., Pilskaln, C., Thunell, R., Pride, C., Sigman, D., Chavez, F., Francois, R., 1999.
772 The nitrogen isotope biogeochemistry of sinking particles from the margin of the Eastern North
773 Pacific. *Deep Sea Research Part I: Oceanographic Research Papers* 46, 655–679.
774 [https://doi.org/10.1016/S0967-0637\(98\)00084-3](https://doi.org/10.1016/S0967-0637(98)00084-3)

775 Amblard, C., 1988. Seasonal succession and strategies of phytoplankton development in two
776 lakes of different trophic states. *J Plankton Res* 10, 1189–1208.
777 <https://doi.org/10.1093/plankt/10.6.1189>

778 Amblard, C., 1986. A study of spatial and temporal variability in the adenine nucleotides of
779 lake phytoplankton during a diel cycle (Lac Pavin, France). *Hydrobiologia* 137, 159–173.
780 <https://doi.org/10.1007/BF00004212>

781 Assayag, N., Jézéquel, D., Ader, M., Viollier, E., Michard, G., Prévot, F., Agrinier, P., 2008.
782 Hydrological budget, carbon sources and biogeochemical processes in Lac Pavin (France):
783 Constraints from $\delta^{18}\text{O}$ of water and $\delta^{13}\text{C}$ of dissolved inorganic carbon. *Applied Geochemistry*
784 23, 2800–2816. <https://doi.org/10.1016/j.apgeochem.2008.04.015>

785 Beaumont, V., Robert, F., 1999. Nitrogen isotope ratios of kerogens in Precambrian cherts: a
786 record of the evolution of atmosphere chemistry? *Precambrian Research* 96, 63–82.
787 [https://doi.org/10.1016/S0301-9268\(99\)00005-4](https://doi.org/10.1016/S0301-9268(99)00005-4)

788 Bebout, G.E., Fogel, M.L., 1992. Nitrogen-isotope compositions of metasedimentary rocks in
789 the Catalina Schist, California: Implications for metamorphic devolatilization history.
790 *Geochimica et Cosmochimica Acta* 56, 2839–2849. [https://doi.org/10.1016/0016-](https://doi.org/10.1016/0016-7037(92)90363-N)
791 [7037\(92\)90363-N](https://doi.org/10.1016/0016-7037(92)90363-N)

792 Bernasconi, S.M., Barbieri, A., Simona, M., 1997. Carbon and nitrogen isotope variations in
793 sedimenting organic matter in Lake Lugano. *Limnology and Oceanography* 42, 1755–1765.

794 Biderre-Petit, C., Boucher, D., Kuever, J., Alberic, P., Jézéquel, D., Chebance, B., Borrel, G.,
795 Fonty, G., Peyret, P., 2011. Identification of Sulfur-Cycle Prokaryotes in a Low-Sulfate Lake
796 (Lake Pavin) Using *aprA* and 16S rRNA Gene Markers. *Microb Ecol* 61, 313–327.
797 <https://doi.org/10.1007/s00248-010-9769-4>

798 Bidaud C.C., Monteil C.L., Menguy N., Busigny V., Jézéquel D., Viollier E., Travert C.,
799 Skouri-Panet F., Benzerara K., Lefevre C.T., Duprat E., 2022. Biogeochemical Niche of
800 Magnetotactic Cocci Capable of Sequestering Large Polyphosphate Inclusions in the Anoxic
801 Layer of the Lake Pavin Water Column. *Frontiers in Microbiology* 12: 789134.
802 <https://doi.org/10.3389/fmicb.2021.789134>

803 Boocock, T.J., Mikhail, S., Boyce, A.J., Prytulak, J., Savage, P.S., Stueeken, E.E., 2023. A
804 primary magmatic source of nitrogen to the Earth's crust. *Nature Geoscience* 16, 521–526,
805 <https://doi.org/10.1038/s41561-023-01194-3>.

806 Borrel, G., Jézéquel, D., Biderre-Petit, C., Morel-Desrosiers, N., Morel, J.-P., Peyret, P., Fonty,
807 G., Lehours, A.-C., 2011. Production and consumption of methane in freshwater lake
808 ecosystems. *Research in Microbiology* 162, 832–847.

809 <https://doi.org/10.1016/j.resmic.2011.06.004>

810 Boudou, J.-P., Schimmelmann, A., Ader, M., Mastalerz, M., Sebilo, M., Gengembre, L., 2008.

811 Organic nitrogen chemistry during low-grade metamorphism. *Geochimica et Cosmochimica*

812 *Acta* 72, 1199–1221. <https://doi.org/10.1016/j.gca.2007.12.004>

813 Bourdier, G., Amblard, C., 1987. Evolution de la composition en acides gras d'un

814 phytoplancton lacustre (Lac Pavin, France). *Int. Revue ges. Hydrobiol. Hydrogr.* 72, 81–95.

815 <https://doi.org/10.1002/iroh.19870720110>

816 Brahney, J., Bos, D.G., Pellatt, M.G., Edwards, T.W.D., Routledge, R., 2006. The influence of

817 nitrogen limitation on d15N and carbon: nitrogen ratios in sediments from sockeye salmon

818 nursery lakes in British Columbia, Canada. *Limnol. Oceanogr.* 51, 2333–2340.

819 <https://doi.org/10.4319/lo.2006.51.5.2333>

820 Brodie, C.R., Leng, M.J., Casford, J.S.L., Kendrick, C.P., Lloyd, J.M., Zong, Y.Q., Bird, M.I.,

821 2011a. Evidence for bias in C and N concentrations and $\delta^{13}\text{C}$ composition of terrestrial and

822 aquatic organic materials due to pre-analysis acid preparation methods. *Chem. Geol.* 282, 67–

823 83.

824 Brodie, C.R., Casford, J.S.L., Lloyd, J.M., Leng, M.J., Heaton, T.H.E., Kendrick, C.P., Zong,

825 Y.Q., 2011b. Evidence for bias in C/N, $\delta^{13}\text{C}$ and $\delta^{15}\text{N}$ values of bulk organic matter, and on

826 environmental interpretation, from a lake sedimentary sequence by pre-analysis acid treatment

827 methods. *Quat. Sci. Rev.* 30, 3076–3087.

828 Bura-Nakić, E., Viollier, E., Jézéquel, D., Thiam, A., Ciglencčki, I., 2009. Reduced sulfur and

829 iron species in anoxic water column of meromictic crater Lake Pavin (Massif Central, France).

830 *Chemical Geology* 266, 311–317. <https://doi.org/10.1016/j.chemgeo.2009.06.020>

831 Bura-Nakić, E., Viollier, E., Ciglencčki, I., 2013. Electrochemical and Colorimetric

832 Measurements Show the Dominant Role of FeS in a Permanently Anoxic Lake. *Environ. Sci.*

833 *Technol.* 47, 741–749. <https://doi.org/10.1021/es303603j>

834 Busigny, V., Ader, M., Cartigny, P., 2005. Quantification and isotopic analysis of nitrogen in

835 rocks at the ppm level using sealed tube combustion technique: A prelude to the study of altered

836 oceanic crust. *Chemical Geology* 223, 249–258.

837 <https://doi.org/10.1016/j.chemgeo.2005.08.002>

838 Busigny, V., Bebout, G.E., 2013. Nitrogen in the Silicate Earth: Speciation and Isotopic

839 Behavior during Mineral-Fluid Interactions. *Elements* 9, 353–358.

840 <https://doi.org/10.2113/gselements.9.5.353>

841 Busigny, V., Jézéquel, D., Cosmidis, J., Viollier, E., Benzerara, K., Planavsky, N.J., Albéric,

842 P., Lebeau, O., Sarazin, G., Michard, G., 2016. The Iron Wheel in Lac Pavin: Interaction with

843 Phosphorus Cycle, in: Sime-Ngando, T., Boivin, P., Chapron, E., Jezequel, D., Meybeck, M.

844 (Eds.), *Lake Pavin*. Springer International Publishing, Cham, pp. 205–220.

845 https://doi.org/10.1007/978-3-319-39961-4_12

846 Busigny, V., Planavsky, N.J., Jézéquel, D., Crowe, S., Louvat, P., Moureau, J., Viollier, E.,

847 Lyons, T.W., 2014. Iron isotopes in an Archean ocean analogue. *Geochimica et Cosmochimica*

848 *Acta* 133, 443–462. <https://doi.org/10.1016/j.gca.2014.03.004>

849 Busigny V., Mathon F.P., Jézéquel D., Bidaud C., Viollier E., Bardoux G., Bourrand J.-J.,

850 Benzerara K., Duprat E., Menguy N., Monteil C.L., Lefevre C.T., 2021. Mass collection of

851 magnetotactic bacteria from the permanently stratified ferruginous Lake Pavin, France.

852 *Environmental Microbiology*, <https://doi.org/10.1111/1462-2920.15458>.

853 Cadeau, P., Ader, M., Jézéquel, D., Chaduteau, C., Sarazin, G., Bernard, C., Leboulanger, C.,

854 2021. Nitrogen Isotope Discrepancy Between Primary Producers and Sediments in an Anoxic

855 and Alkaline Lake. *Front. Earth Sci.* 9, 787386. <https://doi.org/10.3389/feart.2021.787386>

856 Campbell, P., Torgersen, T., 1980. Maintenance of Iron Meromixis by Iron Redeposition in a
857 Rapidly Flushed Monimolimnion. *Can. J. Fish. Aquat. Sci.* 37, 1303–1313.
858 <https://doi.org/10.1139/f80-166>

859 Chapron, E., Albéric, P., Jézéquel, D., Versteeg, W., Bourdier, J.-L., Sitbon, J., 2010.
860 Multidisciplinary characterisation of sedimentary processes in a recent maar lake (Lake Pavin,
861 French Massif Central) and implication for natural hazards. *Nat. Hazards Earth Syst. Sci.* 10,
862 1815–1827. <https://doi.org/10.5194/nhess-10-1815-2010>

863 Chen, F., Zhang, L., Yang, Y., Zhang, D., 2008. Chemical and isotopic alteration of organic
864 matter during early diagenesis: Evidence from the coastal area off-shore the Pearl River estuary,
865 south China. *Journal of Marine Systems* 74, 372–380.
866 <https://doi.org/10.1016/j.jmarsys.2008.02.004>

867 Cheng, C., Busigny, V., Ader, M., Thomazo, C., Chaduteau, C., Philippot, P., 2019. Nitrogen
868 isotope evidence for stepwise oxygenation of the ocean during the Great Oxidation Event.
869 *Geochimica et Cosmochimica Acta* 261, 224–247. <https://doi.org/10.1016/j.gca.2019.07.011>

870 Clement, J.C., Shrestha, J., Ehrenfeld, J.G., Jaffe, P.R., 2005. Ammonium oxidation coupled to
871 dissimilatory reduction of iron under anaerobic conditions in wetland soils. *Soil Biology and*
872 *Biochemistry* 37, 2323–2328.

873 Cosmidis, J., Benzerara, K., Morin, G., Busigny, V., Lebeau, O., Jézéquel, D., Noël, V., Dublet,
874 G., Othmane, G., 2014. Biomineralization of iron-phosphates in the water column of Lake
875 Pavin (Massif Central, France). *Geochimica et Cosmochimica Acta* 126, 78–96.
876 <https://doi.org/10.1016/j.gca.2013.10.037>

877 Fogel, M.L., Cifuentes, L.A., 1993. Isotope Fractionation during Primary Production, in: Engel,
878 M.H., Macko, S.A. (Eds.), *Organic Geochemistry, Topics in Geobiology*. Springer US, Boston,
879 MA, pp. 73–98. https://doi.org/10.1007/978-1-4615-2890-6_3

880 Freudenthal, T., Wagner, T., Wenzhöfer, F., Zabel, M., Wefer, G., 2001. Early diagenesis of
881 organic matter from sediments of the eastern subtropical Atlantic: evidence from stable nitrogen
882 and carbon isotopes. *Geochimica et Cosmochimica Acta* 65, 1795–1808.
883 [https://doi.org/10.1016/S0016-7037\(01\)00554-3](https://doi.org/10.1016/S0016-7037(01)00554-3)

884 Fulton, J.M., Arthur, M.A., Freeman, K.H., 2012. Black Sea nitrogen cycling and the
885 preservation of phytoplankton $\delta^{15}\text{N}$ signals during the Holocene. *Global Biogeochem. Cycles*
886 26, n/a-n/a. <https://doi.org/10.1029/2011GB004196>

887 Galbraith, E.D., Sigman, D.M., Robinson, R.S., Pedersen, Thomas.F., 2008. Nitrogen in Past
888 Marine Environments, in: *Nitrogen in the Marine Environment*. Elsevier, pp. 1497–1535.
889 <https://doi.org/10.1016/B978-0-12-372522-6.00034-7>

890 Garvin, J., Buick, R., Anbar, A.D., Arnold, G.L., Kaufman, A.J., 2009. Isotopic Evidence for
891 an Aerobic Nitrogen Cycle in the Latest Archean. *Science* 323, 1045–1048.
892 <https://doi.org/10.1126/science.1165675>

893 Gaye, B., Wiesner, M.G., Lahajnar, N., 2009. Nitrogen sources in the South China Sea, as
894 discerned from stable nitrogen isotopic ratios in rivers, sinking particles, and sediments. *Marine*
895 *Chemistry* 114, 72–85. <https://doi.org/10.1016/j.marchem.2009.04.003>

896 Godfrey, L.V., Falkowski, P.G., 2009. The cycling and redox state of nitrogen in the Archean
897 ocean. *Nature Geosci* 2, 725–729. <https://doi.org/10.1038/ngeo633>

898 Gonfiantini, R., Stichler, W., Rozanski, K., 1995. Standards and intercomparison materials
899 distributed by the International Atomic Energy Agency for stable isotope measurements,
900 Reference and Intercomparison Materials for Stable Isotopes of Light Elements, IAEA-
901 TECDOC-825.

902 Grami, B., Rasconi, S., Niquil, N., Jobard, M., Saint-Béat, B., Sime-Ngando, T., 2011.

903 Functional effects of parasites on food web properties during the spring diatom bloom in Lake
904 Pavin: A linear inverse modeling analysis. *PLoS ONE* 6, e23273.
905 <https://doi.org/10.1371/journal.pone.0023273>

906 Granger, J., Sigman, D.M., 2009. Removal of nitrite with sulfamic acid for nitrate N and O
907 isotope analysis with the denitrifier method. *Rapid Commun. Mass Spectrom.* 23, 3753–3762.

908 Gu, B., Schelske, L., 1996. Temporal and spatial variations in phytoplankton carbon isotopes
909 in a polymictic subtropical lake. *J Plankton Res* 18, 2081–2092.
910 <https://doi.org/10.1093/plankt/18.11.2081>

911 Hadas, O., Altabet, M.A., Agnihotri, R., 2009. Seasonally varying nitrogen isotope
912 biogeochemistry of particulate organic matter in Lake Kinneret, Israel. *Limnol. Oceanogr.* 54,
913 75–85. <https://doi.org/10.4319/lo.2009.54.1.0075>

914 Hashizume, K., Pinti, D.L., Orberger, B., Cloquet, C., Jayananda, M., Soyama, H., 2016. A
915 biological switch at the ocean surface as a cause of laminations in a Precambrian iron formation.
916 *Earth and Planetary Science Letters* 446, 27–36. <https://doi.org/10.1016/j.epsl.2016.04.023>

917 Jenkyns, H.C., Matthews, A., Tsikos, H., Erel, Y., 2007. Nitrate reduction, sulfate reduction,
918 and sedimentary iron isotope evolution during the Cenomanian-Turonian oceanic anoxic event.
919 *Paleoceanography* 22, n/a-n/a. <https://doi.org/10.1029/2006PA001355>

920 Jézéquel, D., Michard, G., Viollier, E., Agrinier, P., Albéric, P., Lopes, F., Abril, G.,
921 Bergonzini, L., 2016. Carbon Cycle in a Meromictic Crater Lake: Lake Pavin, France, in: Sime-
922 Ngando, T., Boivin, P., Chapron, E., Jezequel, D., Meybeck, M. (Eds.), *Lake Pavin*. Springer
923 International Publishing, Cham, pp. 185–203. https://doi.org/10.1007/978-3-319-39961-4_11

924 Junium, C.K., Arthur, M.A., 2007. Nitrogen cycling during the Cretaceous, Cenomanian-
925 Turonian Oceanic Anoxic Event II. *Geochem. Geophys. Geosyst.* 8, n/a-n/a.
926 <https://doi.org/10.1029/2006GC001328>

927 Juvigné, E., Gewalt, M., 1987. La Narse d'Amboise comme téphrostratotype dans la Chaîne des
928 Puys méridionale (France). *quaternaire* 24, 37–48. <https://doi.org/10.3406/quaternaire.1987.1830>

929 Karhu, J.A., Holland, H.D., 1996. Carbon isotopes and the rise of atmospheric oxygen. *Geol*
930 24, 867. [https://doi.org/10.1130/0091-7613\(1996\)024<0867:CIATRO>2.3.CO;2](https://doi.org/10.1130/0091-7613(1996)024<0867:CIATRO>2.3.CO;2)

931 Kipp, M.A., Stüeken, E.E., Yun, M., Bekker, A., Buick, R., 2018. Pervasive aerobic nitrogen
932 cycling in the surface ocean across the Paleoproterozoic Era. *Earth and Planetary Science*
933 *Letters* 500, 117–126. <https://doi.org/10.1016/j.epsl.2018.08.007>

934 Koehler, M.C., Buick, R., Barley, M.E., 2019. Nitrogen isotope evidence for anoxic deep
935 marine environments from the Mesoproterozoic Mosquito Creek Formation, Australia.
936 *Precambrian Research* 320, 281–290. <https://doi.org/10.1016/j.precamres.2018.11.008>

937 Kohzu, A., Imai, A., Miyajima, T., Fukushima, T., Matsushige, K., Komatsu, K., Kawasaki,
938 N., Miura, S., Sato, T., 2011a. Direct evidence for nitrogen isotope discrimination during
939 sedimentation and early diagenesis in Lake Kasumigaura, Japan. *Organic Geochemistry* 42,
940 173–183. <https://doi.org/10.1016/j.orggeochem.2010.10.010>

941 Kohzu, A., Imai, A., Ohkouchi, N., Fukushima, T., Kamiya, K., Komatsu, K., Tomioka, N.,
942 Kawasaki, N., Miura, S., Satou, T., 2011b. Direct evidence for the alteration of ¹³C natural
943 abundances during early diagenesis in Lake Kasumigaura, Japan. *Geochem. Geophys. Geosyst.*
944 12, n/a-n/a. <https://doi.org/10.1029/2011GC003532>

945 Kump, L.R., Junium, C., Arthur, M.A., Brasier, A., Fallick, A., Melezhik, V., Lepland, A.,
946 Černe, A.E., Luo, G., 2011. Isotopic Evidence for Massive Oxidation of Organic Matter
947 Following the Great Oxidation Event. *Science* 334, 1694–1696.
948 <https://doi.org/10.1126/science.1213999>

949 Lehmann, M.F., Bernasconi, S.M., Barbieri, A., McKenzie, J.A., 2002. Preservation of organic

950 matter and alteration of its carbon and nitrogen isotope composition during simulated and in
951 situ early sedimentary diagenesis. *Geochimica et Cosmochimica Acta* 66, 3573–3584.
952 [https://doi.org/10.1016/S0016-7037\(02\)00968-7](https://doi.org/10.1016/S0016-7037(02)00968-7)

953 Lehours, A.-C., Bardot, C., Thenot, A., Debroas, D., Fonty, G., 2005. Anaerobic Microbial
954 Communities in Lake Pavin, a Unique Meromictic Lake in France. *Appl Environ Microbiol* 71,
955 7389–7400. <https://doi.org/10.1128/AEM.71.11.7389-7400.2005>

956 Lehours, A.-C., Evans, P., Bardot, C., Joblin, K., Gérard, F., 2007. Phylogenetic Diversity of
957 Archaea and Bacteria in the Anoxic Zone of a Meromictic Lake (Lake Pavin, France). *Appl*
958 *Environ Microbiol* 73, 2016–2019. <https://doi.org/10.1128/AEM.01490-06>

959 Lehours, A.-C., Batisson, I., Guedon, Mailhot, G., Fonty, G., 2009. Diversity of Culturable
960 Bacteria, from the Anaerobic Zone of the Meromictic Lake Pavin, Able to Perform
961 Dissimilatory-Iron Reduction in Different in Vitro Conditions. *Geomicrobiology journal* 26,
962 212–223.

963 Li, L., Lollar, B.S., Li, H., Wortmann, U.G., Lacrampe-Couloume, G., 2012. Ammonium
964 stability and nitrogen isotope fractionations for $\text{-NH}_3(\text{aq})\text{-NH}_3(\text{gas})$ systems at 20–70°C and
965 pH of 2–13: Applications to habitability and nitrogen cycling in low-temperature hydrothermal
966 systems. *Geochimica et Cosmochimica Acta* 84, 280–296.
967 <https://doi.org/10.1016/j.gca.2012.01.040>

968 Lopes, F., Viollier, E., Thiam, A., Michard, G., Abril, G., Groleau, A., Prévot, F., Carrias, J.-
969 F., Albéric, P., Jézéquel, D., 2011. Biogeochemical modelling of anaerobic vs. aerobic methane
970 oxidation in a meromictic crater lake (Lake Pavin, France). *Applied Geochemistry* 26, 1919–
971 1932. <https://doi.org/10.1016/j.apgeochem.2011.06.021>

972 Luo, G., Junium, C.K., Izon, G., Ono, S., Beukes, N.J., Algeo, T.J., Cui, Y., Xie, S., Summons,
973 R.E., 2018. Nitrogen fixation sustained productivity in the wake of the Palaeoproterozoic Great
974 Oxygenation Event. *Nat Commun* 9, 978. <https://doi.org/10.1038/s41467-018-03361-2>

975 McIlvin, M.R., Altabet, M.A., 2005. Chemical conversion of nitrate and nitrite to nitrous oxide
976 for nitrogen and oxygen isotopic analysis in freshwater and seawater. *Anal. Chem.* 77, 5589–
977 5595.

978 Meyers, P.A., 1994. Preservation of elemental and isotopic source identification of sedimentary
979 organic matter. *Chemical Geology* 114, 289–302. [https://doi.org/10.1016/0009-2541\(94\)90059-0](https://doi.org/10.1016/0009-2541(94)90059-0)

981 Michard, G., Viollier, E., Jézéquel, D., Sarazin, G., 1994. Geochemical study of a crater lake:
982 Pavin Lake, France — Identification, location and quantification of the chemical reactions in
983 the lake. *Chemical Geology* 115, 103–115. [https://doi.org/10.1016/0009-2541\(94\)90147-3](https://doi.org/10.1016/0009-2541(94)90147-3)

984 Michiels, C.C., Darchambeau, F., Roland, F.A., Morana, C., Lliros, M., García-Armisen, T.,
985 Thamdrup, B., Borges, A.V., Canfield, D.E., Servais, P., Descy, J.-P., Crowe, S.A., 2017. Iron-
986 dependent nitrogen cycling in a ferruginous lake and the nutrient status of Proterozoic oceans.
987 *Nature Geoscience* 10, 217–221. <https://doi-org.insu.bib.cnrs.fr/10.1038/ngeo2886>

988 Minagawa, M., Wada, E., 1986. Nitrogen isotope ratios of red tide organisms in the East China
989 Sea: A characterization of biological nitrogen fixation. *Marine Chemistry* 19, 245–259.
990 [https://doi.org/10.1016/0304-4203\(86\)90026-5](https://doi.org/10.1016/0304-4203(86)90026-5)

991 Mingram, B., Bräuer, K., 2001. Ammonium concentration and nitrogen isotope composition in
992 metasedimentary rocks from different tectonometamorphic units of the European Variscan Belt.
993 *Geochimica et Cosmochimica Acta* 65, 273–287. [https://doi.org/10.1016/S0016-7037\(00\)00517-2](https://doi.org/10.1016/S0016-7037(00)00517-2)

995 Möbius, J., 2013. Isotope fractionation during nitrogen remineralization (ammonification):
996 Implications for nitrogen isotope biogeochemistry. *Geochimica et Cosmochimica Acta* 105,

997 422–432. <https://doi.org/10.1016/j.gca.2012.11.048>

998 Möbius, J., Lahajnar, N., Emeis, K.-C., 2010. Diagenetic control of nitrogen isotope ratios in
999 Holocene sapropels and recent sediments from the Eastern Mediterranean Sea. *Biogeosciences*
1000 7, 3901–3914. <https://doi.org/10.5194/bg-7-3901-2010>

1001 Müller, P.J., 1977. C/N ratios in Pacific deep-sea sediments: Effect of inorganic ammonium
1002 and organic nitrogen compounds sorbed by clays. *Geochimica et Cosmochimica Acta* 41, 765-
1003 776.

1004 Pinti, D.L., Hashizume, K., Matsuda, J., 2001. Nitrogen and argon signatures in 3.8 to 2.8 Ga
1005 metasediments: clues on the chemical state of the archaic ocean and the deep biosphere.
1006 *Geochimica et Cosmochimica Acta* 65, 2301–2315. [https://doi.org/10.1016/S0016-7037\(01\)00590-7](https://doi.org/10.1016/S0016-7037(01)00590-7)

1008 Pinti, D.L., Hashizume, K., Sugihara, A., Massault, M., Philippot, P., 2009. Isotopic
1009 fractionation of nitrogen and carbon in Paleoarchaic cherts from Pilbara craton, Western
1010 Australia: Origin of ^{15}N -depleted nitrogen. *Geochimica et Cosmochimica Acta* 73, 3819–3848.
1011 <https://doi.org/10.1016/j.gca.2009.03.014>

1012 Prah, F.G., Cowie, G.L., De Lange, G.J., Sparrow, M.A., 2003. Selective organic matter
1013 preservation in “burn-down” turbidites on the Madeira Abyssal Plain: SELECTIVE
1014 PRESERVATION. *Paleoceanography* 18, n/a-n/a. <https://doi.org/10.1029/2002PA000853>

1015 Prokopenko, M.G., Hammond, D.E., Berelson, W.M., Bernhard, J.M., Stott, L., Douglas, R.,
1016 2006. Nitrogen cycling in the sediments of Santa Barbara basin and Eastern Subtropical North
1017 Pacific: Nitrogen isotopes, diagenesis and possible chemosymbiosis between two lithotrophs
1018 (*Thioploca* and *Anammox*)— “riding on a glider”. *Earth and Planetary Science Letters* 242,
1019 186-204.

1020 Quan, T.M., Adeboye, O.O., 2021. Interpretation of Nitrogen Isotope Profiles in Petroleum
1021 Systems: A Review. *Front. Earth Sci.* 9, 705691. <https://doi.org/10.3389/feart.2021.705691>

1022 Quan, T.M., Falkowski, P.G., 2009. Redox control of N:P ratios in aquatic ecosystems.
1023 *Geobiology* 7, 124–139. <https://doi.org/10.1111/j.1472-4669.2008.00182.x>

1024 Quan, T.M., Wright, J.D., Falkowski, P.G., 2013. Co-variation of nitrogen isotopes and redox
1025 states through glacial–interglacial cycles in the Black Sea. *Geochimica et Cosmochimica Acta*
1026 112, 305–320. <https://doi.org/10.1016/j.gca.2013.02.029>

1027 Rau, G.H., Arthur, M.A., Dean, W.E., 1987. $^{15}\text{N}/^{14}\text{N}$ variations in Cretaceous Atlantic
1028 sedimentary sequences: implication for past changes in marine nitrogen biogeochemistry. *Earth*
1029 *and Planetary Science Letters* 82, 269–279. [https://doi.org/10.1016/0012-821X\(87\)90201-9](https://doi.org/10.1016/0012-821X(87)90201-9)

1030 Restituto, F., 1984. Contribution à l'étude du sédiment d'un lac oligomésotrophe d'origine
1031 volcanique (Lac Pavin, France). *Hydrobiologia* 109, 229–234.
1032 <https://doi.org/10.1007/BF00007740>

1033 Riebesell, U., Burkhardt, S., Dauelsberg, A., Kroon, B., 2000. Carbon isotope fractionation by
1034 a marine diatom: dependence on the growth-rate-limiting resource. *Mar. Ecol. Prog. Ser.* 193,
1035 295–303. <https://doi.org/10.3354/meps193295>

1036 Robinson, R.S., Kienast, M., Luiza Albuquerque, A., Altabet, M., Contreras, S., De Pol Holz,
1037 R., Dubois, N., Francois, R., Galbraith, E., Hsu, T.-C., Ivanochko, T., Jaccard, S., Kao, S.-J.,
1038 Kiefer, T., Kienast, S., Lehmann, M., Martinez, P., McCarthy, M., Möbius, J., Pedersen, T.,
1039 Quan, T.M., Ryabenko, E., Schmittner, A., Schneider, R., Schneider-Mor, A., Shigemitsu, M.,
1040 Sinclair, D., Somes, C., Studer, A., Thunell, R., Yang, J.-Y., 2012. A review of nitrogen isotopic
1041 alteration in marine sediments. *Paleoceanography* 27. <https://doi.org/10.1029/2012PA002321>

1042 Sachs, J.P., Repeta, D.J., 1999. Oligotrophy and Nitrogen Fixation During Eastern
1043 Mediterranean Sapropel Events. *Science* 286, 2485–2488.

1044 <https://doi.org/10.1126/science.286.5449.2485>

1045 Schettler, G., Schwab, M.J., Stebich, M., 2007. A 700-year record of climate change based on
1046 geochemical and palynological data from varved sediments (Lac Pavin, France). *Chemical*
1047 *Geology* 240, 11–35. <https://doi.org/10.1016/j.chemgeo.2007.01.003>

1048 Sigman, D.M., Karsh, K.L., Casciotti, K.L., 2009. Nitrogen Isotopes in the Ocean, in:
1049 *Encyclopedia of Ocean Sciences*. Elsevier, pp. 40–54. [https://doi.org/10.1016/B978-](https://doi.org/10.1016/B978-012374473-9.00632-9)
1050 [012374473-9.00632-9](https://doi.org/10.1016/B978-012374473-9.00632-9)

1051 Stebich, M., Brüchmann, C., Kulbe, T., Negendank, J.F.W., 2005. Vegetation history, human
1052 impact and climate change during the last 700 years recorded in annually laminated sediments
1053 of Lac Pavin, France. *Review of Palaeobotany and Palynology* 133, 115–133.
1054 <https://doi.org/10.1016/j.revpalbo.2004.09.004>

1055 Stüeken, E.E., Buick, R., 2018. Environmental control on microbial diversification and methane
1056 production in the Mesoarchean. *Precambrian Research* 304, 64–72.
1057 <https://doi.org/10.1016/j.precamres.2017.11.003>

1058 Stüeken, Eva E., Buick, R., Guy, B.M., Koehler, M.C., 2015. Isotopic evidence for biological
1059 nitrogen fixation by molybdenum-nitrogenase from 3.2 Gyr. *Nature* 520, 666–669.
1060 <https://doi.org/10.1038/nature14180>

1061 Stüeken, E.E., Buick, R., Schauer, A.J., 2015. Nitrogen isotope evidence for alkaline lakes on
1062 late Archean continents. *Earth and Planetary Science Letters* 411, 1–10.
1063 <https://doi.org/10.1016/j.epsl.2014.11.037>

1064 Stüeken, E.E., Kipp, M.A., Koehler, M.C., Buick, R., 2016. The evolution of Earth's
1065 biogeochemical nitrogen cycle. *Earth-Science Reviews* 160, 220–239.
1066 <https://doi.org/10.1016/j.earscirev.2016.07.007>

1067 Thomazo, C., Ader, M., Philippot, P., 2011. Extreme ¹⁵N-enrichments in 2.72-Gyr-old
1068 sediments: evidence for a turning point in the nitrogen cycle. *Geobiology* 9, 107–120.
1069 <https://doi.org/10.1111/j.1472-4669.2011.00271.x>

1070 Thomazo, C., Papineau, D., 2013. Biogeochemical cycling of nitrogen on the early Earth.
1071 *Elements* 9, 345–351. <https://doi.org/10.2113/gselements.9.5.345>

1072 Thunell, R.C., Sigman, D.M., Muller-Karger, F., Astor, Y., Varela, R., 2004. Nitrogen isotope
1073 dynamics of the Cariaco Basin, Venezuela. *Global Biogeochem. Cycles* 18, n/a-n/a.
1074 <https://doi.org/10.1029/2003GB002185>

1075 Ueno, Y., Yamada, K., Yoshida, N., Maruyama, S., Isozaki, Y., 2006. Evidence from fluid
1076 inclusions for microbial methanogenesis in the early Archaean era. *Nature* 440, 516–519.
1077 <https://doi.org/10.1038/nature04584>

1078 Vargas, M., Kashefi, K., Blunt-Harris, E.L., Lovley, D.R., 1998. Microbiological evidence for
1079 Fe(III) reduction on early Earth. *Nature* 395, 65–67. <https://doi.org/10.1038/25720>

1080 Velinsky, D.J., Fogel, M.L., 1999. Cycling of dissolved and particulate nitrogen and carbon in
1081 the Framvaren Fjord, Norway: stable isotopic variations. *Marine Chemistry* 67, 161–180.
1082 [https://doi.org/10.1016/S0304-4203\(99\)00057-2](https://doi.org/10.1016/S0304-4203(99)00057-2)

1083 Velinsky, D.J., Fogel, M.L., Todd, J.F., Tebo, B.M., 1991. Isotopic fractionation of dissolved
1084 ammonium at the oxygen-hydrogen sulfide interface in anoxic waters. *Geophys. Res. Lett.* 18,
1085 649–652. <https://doi.org/10.1029/91GL00344>

1086 Viollier, E., Jézéquel, D., Michard, G., Pèpe, M., Sarazin, G., Alberic, P., 1995. Geochemical
1087 study of a crater lake (Pavin Lake, France): Trace-element behaviour in the monimolimnion.
1088 *Chemical Geology* 125, 61–72. [https://doi.org/10.1016/0009-2541\(95\)00059-U](https://doi.org/10.1016/0009-2541(95)00059-U)

1089 Viollier, E., Michard, G., Jézéquel, D., Pèpe, M., Sarazin, G., 1997. Geochemical study of a
1090 crater lake: Lake Pavin, Puy de Dôme, France. Constraints afforded by the particulate matter

1091 distribution in the element cycling within the lake. *Chemical Geology* 142, 225–241.
1092 [https://doi.org/10.1016/S0009-2541\(97\)00093-4](https://doi.org/10.1016/S0009-2541(97)00093-4)

1093 Yang, W.H., Weber, K.A., Silver, W.L., 2012. Nitrogen loss from soil through anaerobic
1094 ammonium oxidation coupled to iron reduction. *Nature Geoscience* 5, 538–541.

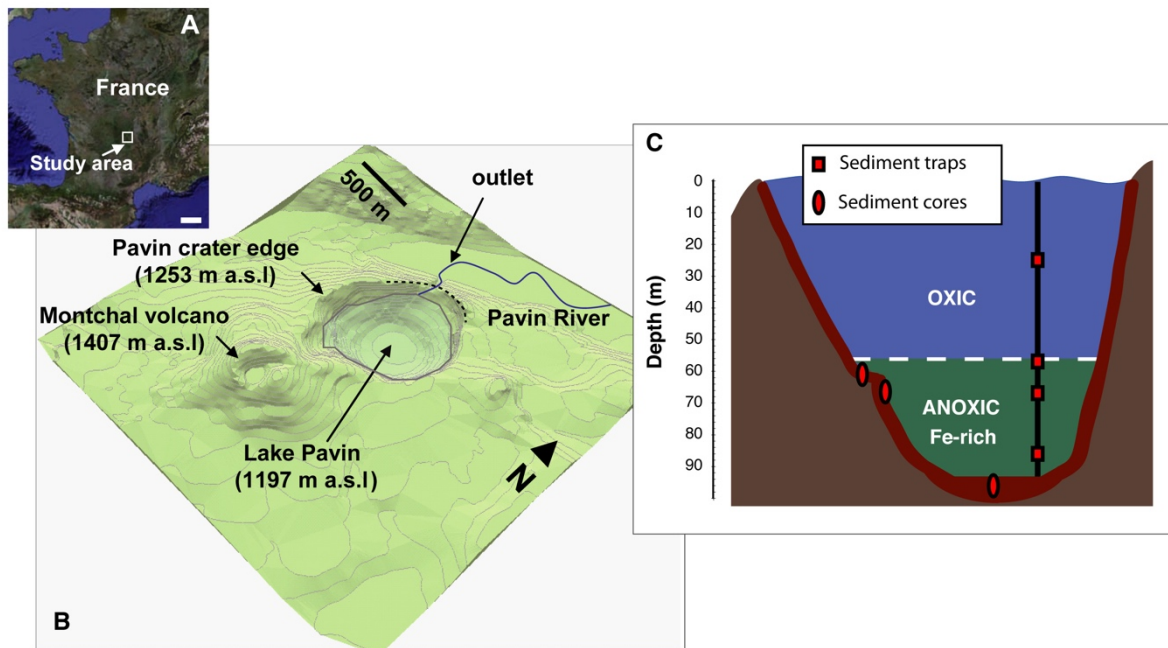
1095 Zerkle, A.L., Junium, C.K., Canfield, D.E., House, C.H., 2008. Production of ¹⁵N-depleted
1096 biomass during cyanobacterial N₂-fixation at high Fe concentrations. *J. Geophys. Res.* 113,
1097 G03014. <https://doi.org/10.1029/2007JG000651>

1098 Zerkle, A.L., Poulton, S.W., Newton, R.J., Mettam, C., Claire, M.W., Bekker, A., Junium, C.K.,
1099 2017. Onset of the aerobic nitrogen cycle during the Great Oxidation Event. *Nature* 542, 465–
1100 467. <https://doi.org/10.1038/nature20826>

1101 Zhang, X., Sigman, D.M., Morel, F.M.M., Kraepiel, A.M.L., 2014. Nitrogen isotope
1102 fractionation by alternative nitrogenases and past ocean anoxia. *Proc. Natl. Acad. Sci. U.S.A.*
1103 111, 4782–4787. <https://doi.org/10.1073/pnas.1402976111>

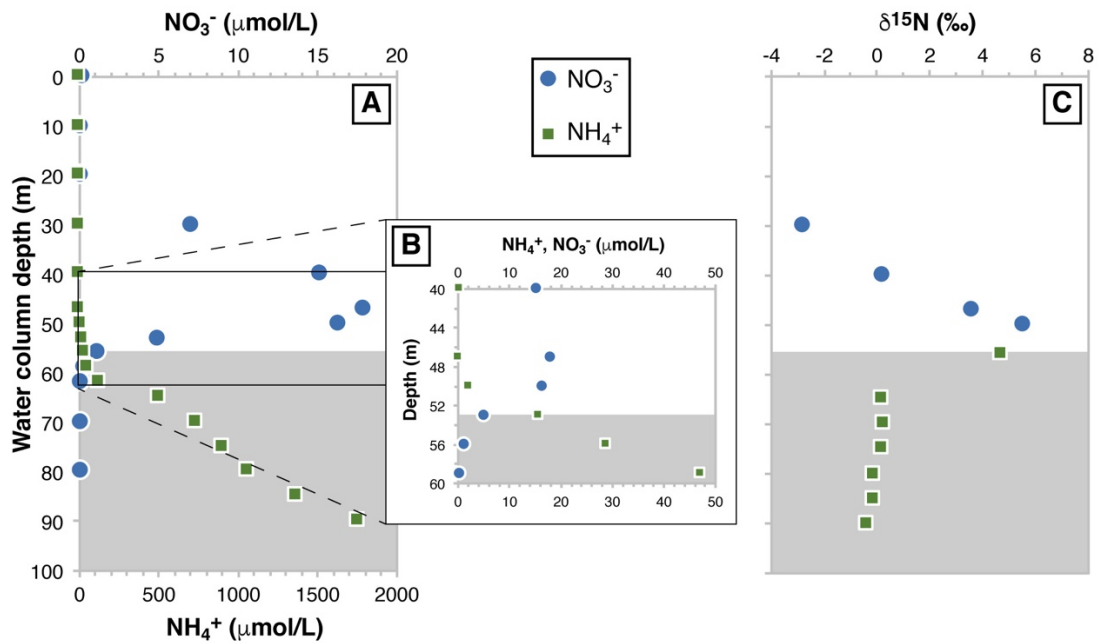
1104
1105
1106
1107
1108
1109

1110
1111



1112
1113
1114
1115
1116
1117
1118
1119
1120

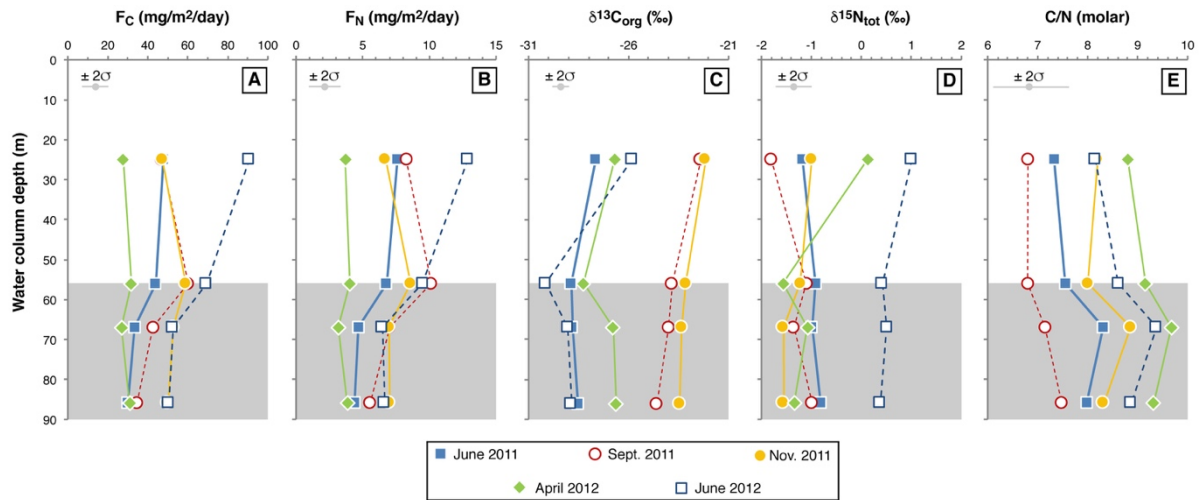
Fig. 1. (A) Location of Lake Pavin, France (scale given by the white bar, representing 100 km). (B) Elevation/bathymetric map showing the main features of Lake Pavin area. (C) Schematic representation of Lake Pavin and the samples studied here: 4 sediment traps in the oxic (25 and 56 m depth) and anoxic (67 and 86 m) zones, as well as 3 sediment cores from the anoxic zone. Figures A and B are modified from Chapron *et al.* (2010).



1121
1122
1123
1124
1125

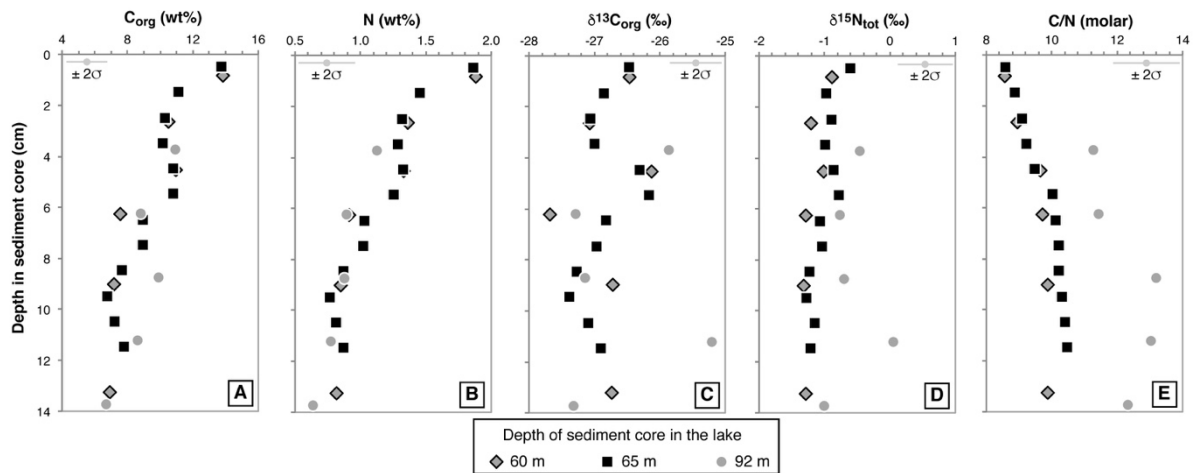
Fig. 2. Dissolved nitrate (circles) and ammonium (squares) concentrations (A) and isotope compositions (B) in lake Pavin water column. (A) nitrate and ammonium concentrations, (B) zoom in the redox transition zone, (C) nitrogen isotope compositions. Note the different scales for nitrate and ammonium concentrations in figure A. The grey area represents the anoxic zone.

1126
1127



1128
1129
1130
1131
1132
1133
1134
1135
1136
1137

Fig. 3. Organic carbon and nitrogen fluxes (F_C and F_N) and isotope compositions ($\delta^{13}C_{org}$ and $\delta^{15}N_{tot}$), as well as C/N ratios measured in sediment traps collected in Lake Pavin at 5 different periods, from June 2011 to June 2012. The grey area represents the anoxic zone. The error bars correspond to $\pm 2\sigma$.



1138
1139
1140
1141
1142
1143
1144
1145
1146
1147
1148
1149
1150

Fig. 4. Organic carbon and nitrogen concentrations and isotope compositions, as well as C/N ratios measured in the three sediment cores from the anoxic zone of Lake Pavin (see core location in Fig. 1). The three cores were collected near but just below the redox transition zone (60 m), near the peak of sulfate reduction zone (65 m), and at the lake bottom (92 m). The error bars correspond to $\pm 2\sigma$.

1151
1152
1153

Table 1

Dissolved ammonium and nitrate concentrations and isotope composition in Lake Pavin water column.

Depth* (m)	NH ₄ ⁺ (μM)	δ ¹⁵ N _{NH4+} (‰)	NO ₃ ⁻ (μM)	δ ¹⁵ N _{NO3-} (‰)
0	0.2		0.20	
10	0.2		0.01	
20	0.1		0.01	
30	0.1		7.00	-2.8
40	0.2		15.18	0.2
47	0.0		17.85	3.6
50	2.2		16.30	5.5
53	15.7		4.92	
56	28.8	4.70	1.16	
59	47.1		0.29	
62	118		0.09	
65	500	0.22		
70	731	0.27	0.06	
75	900	0.17		
80	1057	-0.13	0.06	
85	1366	-0.12		
90	1753	-0.36		

1154 * Depth in the water column.

1155
1156

1157
1158
1159
1160
1161

Table 2

Organic carbon and nitrogen fluxes (F_C and F_N) and isotope compositions ($\delta^{13}C_{org}$ and $\delta^{15}N_{org}$), as well as C/N ratios, in sediment traps from lake Pavin. All data correspond to the average values and 2SD (standard deviation) of two or three replicate analyses.

Sample	Depth* (m)	F_C $mg.m^{-2}.day^{-1}$	F_N $mg.m^{-2}.day^{-1}$	$\delta^{13}C_{org}$ (‰) $\pm (2\sigma)$	$\delta^{15}N_{org}$ (‰) $\pm (2\sigma)$	C/N $\pm (2\sigma)$
March-June 2011						
MX33-T23P	25	47.8	7.6	-27.6 0.4	-1.2 0.1	7.3 0.3
MX33-T58P	56	43.9	6.8	-28.9 0.1	-0.9 0.2	7.6 0.3
MX33-T70P	67	33.4	4.7	-28.8 0.1	-1.0 0.1	8.3 0.1
MX33-T88P	86	30.0	4.4	-28.5 0.1	-0.8 0.2	8.0 0.3
Mean		38.8	5.9	-28.5	-1.0	7.8
SD (2σ)		16.8	3.1	1.1	0.3	0.9
June-September 2011						
MX34-T23P	25	47.0	8.3	-22.4 0.2	-1.8 0.2	6.8 0.3
MX34-T58P	56	60.2	10.1	-23.8 0.1	-1.1 0.1	6.8 0.1
MX34-T70P	67	42.6	7.0	-24.0 0.2	-1.3 0.1	7.2 0.3
MX34-T88P	86	34.5	5.6	-24.6 0.2	-1.0 0.1	7.5 0.3
Mean		46.1	7.8	-23.7	-1.3	7.1
SD (2σ)		21.5	3.9	1.9	0.7	0.6
September-November 2011						
MX35-T23P	25	47.3	6.7	-22.1 0.3	-1.0 0.1	8.2 0.3
MX35-T58P	56	58.9	8.6	-23.1 0.3	-1.2 0.1	8.0 0.1
MX35-T70P	67	52.9	7.0	-23.3 0.2	-1.6 0.1	8.9 0.2
MX35-T88P	86	50.1	7.0	-23.4 0.3	-1.5 0.0	8.3 0.2
Mean		52.3	7.3	-23.0	-1.3	8.3
SD (2σ)		9.9	1.7	1.2	0.6	0.7
November 2011-April 2012						
MX37-T23P	25	27.5	3.7	-26.7 0.1	0.1 0.1	8.8 0.4
MX37-T58P	56	31.8	4.0	-28.2 0.1	-1.6 0.2	9.2 0.0
MX37-T70P	67	26.8	3.2	-26.8 0.1	-1.1 0.2	9.7 0.2
MX37-T88P	86	30.8	3.9	-26.6 0.0	-1.3 0.1	9.3 0.0
Mean		29.2	3.7	-27.1	-1.0	9.2
SD (2σ)		4.9	0.7	1.6	1.5	0.7
April-June 2012						
MX38-T23P	25	90.7	12.9	-25.8 0.1	1.0 0.1	8.2 0.3
MX38-T58P	56	69.4	9.5	-30.1 0.2	0.4 0.3	8.6 0.2
MX38-T70P	67	52.7	6.5	-29.0 0.1	0.5 0.2	9.4 0.1
MX38-T88P	86	50.5	6.6	-28.9 0.0	0.4 0.0	8.9 0.2
Mean		65.8	8.9	-28.5	0.6	8.8
SD (2σ)		37.3	6.0	3.7	0.6	1.0

* Depth in the water column.

1162
1163
1164
1165
1166
1167
1168
1169
1170
1171
1172

1173
1174
1175
1176

Table 3

Organic carbon and nitrogen concentrations and isotope compositions, as well as C/N ratios, in the samples of the three sediment cores from Lake Pavin. All data correspond to the average values and 2SD (standard deviation) of two or three replicate analyses.

Sample	Depth* (cm)	C _{org} %		N _{tot} %		δ ¹³ C _{org} (‰)		δ ¹⁵ N _{tot} (‰)		C/N	
		± (2σ)		± (2σ)		± (2σ)		± (2σ)		± (2σ)	
Core C1 60m											
B2	0.9	13.8	1.3	1.9	0.1	-26.5	0.0	-0.9	0.0	8.6	0.5
D2	2.7	10.5	0.8	1.4	0.0	-27.1	0.1	-1.2	0.1	9.0	0.4
F2	4.6	11.0	0.8	1.3	0.0	-26.1	0.1	-1.0	0.1	9.6	0.6
H2	6.3	7.6	0.9	0.9	0.1	-27.7	0.2	-1.3	0.2	9.7	0.5
I2	9.0	7.2	0.4	0.8	0.0	-26.7	0.0	-1.3	0.2	9.9	0.3
L2	13.3	6.9	0.2	0.8	0.0	-26.7	0.2	-1.3	0.1	9.9	0.2
Mean		9.5		1.2		-26.8		-1.2		9.4	
SD (2σ)		5.5		0.8		1.1		0.4		1.1	
Core C2 65m											
C2-1-1	0.5	13.8	0.9	1.9	0.0	-26.5	0.1	-0.6	0.0	8.6	0.6
C2-2-1	1.5	11.1	0.9	1.5	0.0	-26.8	0.1	-1.1	0.1	8.9	0.6
C2-3-1	2.5	10.3	0.9	1.3	0.1	-27.0	0.0	-0.9	0.0	9.1	0.8
C2-4-1	3.5	10.2	0.7	1.3	0.0	-27.0	0.1	-1.0	0.1	9.2	0.7
C2-5-1	4.5	10.8	1.0	1.3	0.0	-26.3	0.1	-0.8	0.0	9.5	0.8
C2-6-1	5.5	10.8	0.2	1.3	0.1	-26.2	0.0	-0.8	0.1	10.0	1.2
C2-7-1	6.5	9.0	0.1	1.0	0.1	-26.8	0.2	-1.1	0.0	10.1	1.1
C2-8-1	7.5	9.0	0.2	1.0	0.1	-27.0	0.0	-1.0	0.0	10.2	1.2
C2-9-1	8.5	7.7	0.1	0.9	0.1	-27.3	0.1	-1.2	0.0	10.2	0.7
C2-10-1	9.5	6.8	0.9	0.8	0.2	-27.4	0.4	-1.3	0.1	10.3	0.8
C2-11-1	10.5	7.3	0.3	0.8	0.1	-27.1	0.0	-1.1	0.1	10.4	0.7
C2-12-1	11.5	7.8	0.1	0.9	0.1	-26.9	0.1	-1.2	0.2	10.5	1.0
Mean		9.6		1.2		-26.8		-1.0		9.8	
SD (2σ)		4.0		0.6		0.7		0.4		1.3	
Core C6 92m											
1-1	3.75	11.0		1.1	0.3	-25.8	0.1	-0.5	0.1	11.3	0.6
2-1	6.25	8.8	1.3	0.9	0.0	-27.3	0.5	-0.8	0.1	11.5	0.4
3-1	8.75	9.9	1.5	0.9	0.2	-27.1	0.3	-0.7	0.1	13.2	0.7
4-1	11.25	8.7	2.3	0.8	0.2	-25.2	0.2	0.1	0.2	13.0	0.5
5-1	13.75	6.8	1.3	0.6	0.0	-27.3	0.3	-1.0	0.2	12.3	0.3
Mean		9.0		0.9		-26.5		-0.6		12.3	
SD (2σ)		3.1		0.4		1.9		0.8		1.8	

* Depth in the sediment core.

1177
1178
1179
1180
1181
1182
1183
1184
1185
1186
1187
1188
1189
1190
1191
1192

1193
1194
1195
1196

Table 4

Organic carbon and nitrogen concentrations and isotope compositions, as well as C/N ratios, in the beech leaves, spruce thorns and two litters samples collected on the flanks of Pavin crater lake.

Sample	C _{org} (wt.%)	N _{tot} (wt.%)	δ ¹³ C _{org} (‰)	δ ¹⁵ N _{tot} (‰)	C/N molar
brown leaves	46.3	1.4	-30.3	-6.8	37.7
brown leaves	46.3	1.6	-30.5	-6.8	33.7
brown leaves	44.4	1.1	-31.0	-6.6	46.7
brown leaves	44.2	1.3	-31.3	-6.4	41.2
brown leaves	48.3	1.3	-30.7	-7.0	43.4
<i>Avg (±2SD)</i>	<i>45.9 (±3.3)</i>	<i>1.3 (±0.4)</i>	<i>-30.8 (±0.8)</i>	<i>-6.7 (±0.5)</i>	<i>40.5 (±10.1)</i>
Spruce thorns	26.2	1.3	-30.3	-1.6	23.0
Spruce thorns	27.2	1.2	-28.9	-0.7	27.4
Spruce thorns	24.6	1.0	-30.4	-1.2	29.6
Spruce thorns	27.8	1.1	-29.6	-1.5	30.7
<i>Avg (±2SD)</i>	<i>26.5 (±2.8)</i>	<i>1.1 (±0.3)</i>	<i>-29.8 (±1.4)</i>	<i>-1.2 (±0.8)</i>	<i>27.7 (±6.8)</i>
Litter 1	13.5	0.8	-27.9	-3.1	19.2
Litter 1	14.6	1.2	-27.5	-3.2	14.5
Litter 1	15.6	1.0	-28.3	-3.3	18.5
Litter 1	10.8	0.8	-28.1	-3.1	15.3
Litter 1	12.9	0.9	-27.6	-3.2	17.4
<i>Avg (±2SD)</i>	<i>13.5 (±3.7)</i>	<i>0.9 (±0.3)</i>	<i>-27.9 (±0.6)</i>	<i>-3.2 (±0.1)</i>	<i>17.0 (±4.1)</i>
Litter 2	14.0	1.1	-28.3	-2.6	14.9
Litter 2	15.3	1.0	-28.2	-2.3	17.8
Litter 2	15.0	1.1	-28.7	-2.4	15.8
Litter 2	14.1	1.0	-28.8	-2.4	16.1
Litter 2	15.1	1.0	-28.1	-2.6	16.9
<i>Avg (±2SD)</i>	<i>14.7 (±1.3)</i>	<i>1.1 (±0.1)</i>	<i>-28.4±0.6</i>	<i>-2.4 (±0.3)</i>	<i>16.3 (±2.2)</i>

Avg (±2SD): average values and uncertainties expressed as two standard deviations.

1197
1198
1199

1200
1201
1202
1203

Table 5

Global annual fluxes of organic carbon and nitrogen, their isotope compositions, and C/N ratios in Lake Pavin (data calculated from the sediment traps placed at 4 different depths in the water column).

Depth* (m)	F_C $\text{g.m}^{-2}.\text{year}^{-1}$	F_N $\text{g.m}^{-2}.\text{year}^{-1}$	$\delta^{13}\text{C}_{\text{org}}$ (‰)	$\delta^{15}\text{N}_{\text{org}}$ (‰)	C/N
25	17.8 ± 0.8	2.7 ± 0.1	-25.2 ± 0.2	-0.5 ± 0.1	7.9 ± 0.3
56	18.2 ± 1.0	2.7 ± 0.2	-26.9 ± 0.2	-0.8 ± 0.2	8.1 ± 0.1
67	14.3 ± 0.2	1.9 ± 0.1	-26.4 ± 0.1	-0.9 ± 0.1	8.9 ± 0.2
86	13.6 ± 0.7	1.9 ± 0.1	-26.5 ± 0.1	-0.9 ± 0.1	8.6 ± 0.2

1204 * Depth in the water column.

1205
1206
1207
1208
1209

Supplementary materials

1210 *Excel file attached*

1211
1212

Table S1

1214 Vertical variability of phytoplankton species in Lake Pavin water column in June 1984 (data
1215 compiled from Amblard, 1984, 1986). A cross indicates the presence of the species, while
1216 empty space corresponds to an absence.

1217
1218

Table S2

1220 Seasonal variability of phytoplankton species in the first meters of Lake Pavin upper water
1221 column, in June 1984 (data compiled from Bourdier et al., 1987; Amblard, 1988). A cross
1222 indicates the presence of the species, while empty space corresponds to an absence.

1223
1224

Table S3

1225 Measured temperature, dissolved O₂, pH, specific conductivity (at 25°C), and C isotope
1226 composition of dissolved inorganic carbon in November 2002 and July 2004 (Assayag et al.,
1227 2008). The isotope composition of CO₂ is calculated at every depth from isotope composition
1228 of DIC and temperature using Mook (1974).

1229
1230
1231
1232
1233
1234
1235
1236